

LA-UR-16-21655

Approved for public release; distribution is unlimited.

Definition of Beam Diameter for Electron Beam Welding Title:

Author(s): Burgardt, Paul

Pierce, Stanley W. Dvornak, Matthew John

Intended for: Report

Issued: 2016-03-11



DEFINITION of BEAM DIAMETER For ELECTRON BEAM WELDING

P. Burgardt, MST-6 S.W. Pierce, MET-1 M.J. Dvornak, MST-6

Los Alamos, NM

INTRODUCTION

It is useful to characterize the dimensions of the electron beam during process development for electron beam welding applications. Analysis of the behavior of electron beam welds is simplest when a single number can be assigned to the beam properties that describes the size of the beam spot; this value we generically call the "beam diameter". This approach has worked well for most applications and electron beam welding machines with the weld dimensions (width and depth) correlating well with the beam diameter. However, in recent weld development for a refractory alloy, Ta-10W, welded with a low voltage electron beam machine (LVEB), it was found that the weld dimensions (weld penetration and weld width) did not correlate well with the beam diameter and especially with the experimentally determined sharp focus point. These data suggest that the presently used definition of beam diameter may not be optimal for all applications. The possible reasons for this discrepancy and a suggested possible alternative diameter definition is the subject of this paper.

BEAM DIAMETER - A HISTORICAL PERSPECTIVE

Measurements of the electron density in the beam have been made essentially from the onset of EB welding technology (circa 1965) but the measurement techniques tended to be impractical for use at high beam power. Starting circa 1985 devices based on robust tungsten slits over a Faraday cup electron detector were developed that provide a more practical measurement of the electron distribution in the typical electron beam. This approach will generically be called a Modified Faraday Cup (MFC). Two of the devices that are now commercially available are described in: "Evaluation of Two Devices for Electron Beam Profiling", P. Burgardt and S.W. Pierce, LA-UR-14-28680. These instruments measure the electron density in the beam versus radial position (also called beam profiling herein). A map of the electron density versus position is interesting and is useful at times for understanding specific welding issues. However for simple application of these data to understanding weld geometry, it is most useful to assign a single number to the beam that we generically call the beam diameter.

The proper definition of "diameter" is not uniquely defined because the actual beam made by an electron beam welding machine has a complex shape. It has long been known that the beam is nearly Gaussian in shape especially near to sharp focus. Therefore, the simplest approach to measuring beam diameter is based on the assumption that the beam is described by:

$$J = J_0 \exp(-r^2/\sigma^2)$$

where, J is current density, σ is the Gaussian width parameter and r is radial position. This is often a realistic description of the beam produced by a typical high voltage electron beam (HVEB) machine. Figure 1 shows typical electron density data versus position for a HVEB at 110kV accelerating voltage and a beam current of 7 mA. Figure 1 shows data obtained at sharp focus and for modest overfocus. The blue curves on Figure 1 are least-squares fits of a Gaussian distribution to the raw data. It is apparent that the simple Gaussian assumption is a reasonable description of the beam over a range of focus conditions for a typical HVEB machine.

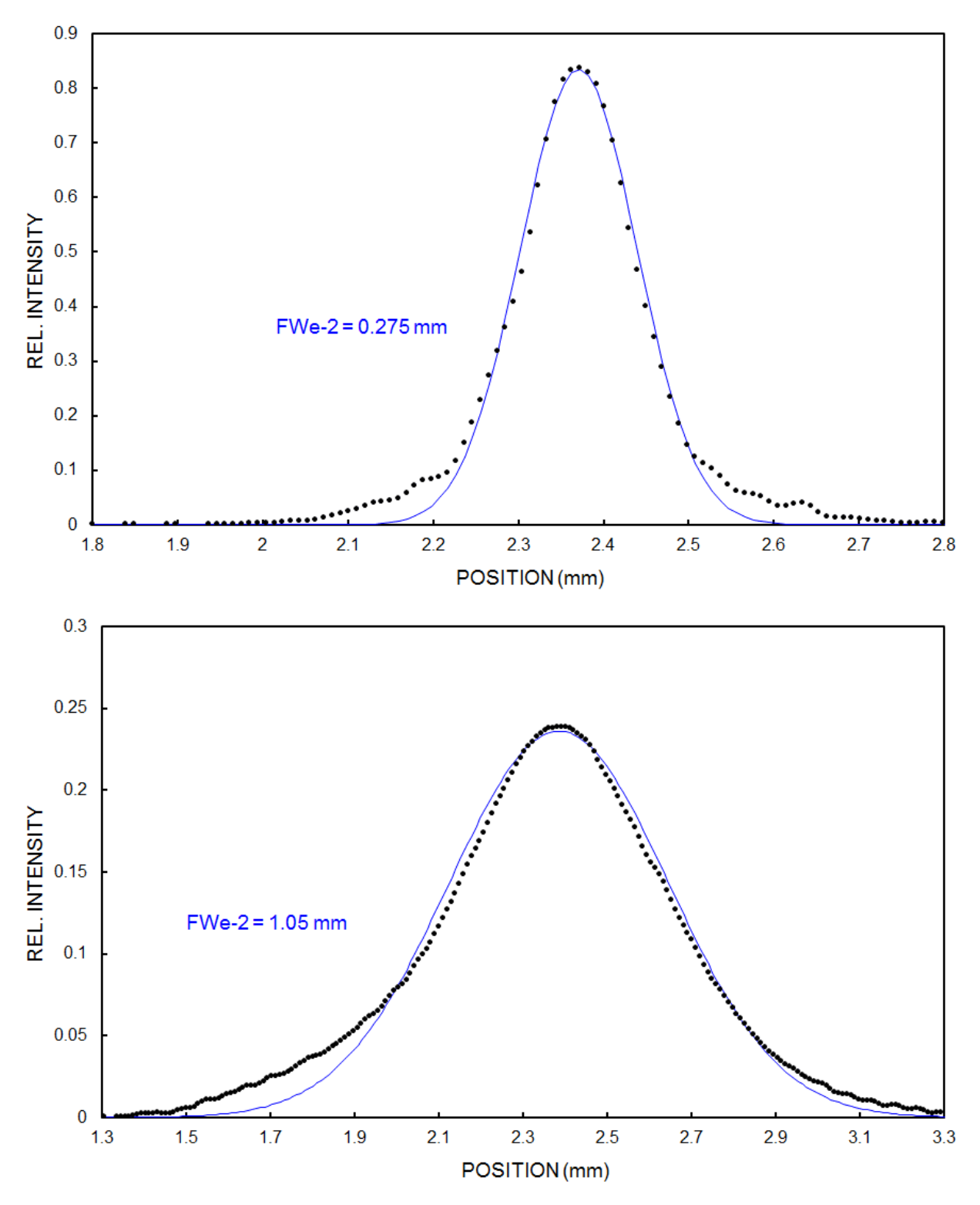


Figure 1: Electron density (arbitrary units) versus radial position for a typical HVEB at 100 kV and 7 mA at sharp focus (the upper data) and for 20 units overfocus (the lower data). The blue curves are least-squares Gaussian fits to the raw data illustrating that the beam is adequately described by a Gaussian distribution over a fairly wide range of conditions.

Based on the notion that the beam is Gaussian, the definition of beam diameter might be based on a measurement of the beam width parameter, σ . Historically there have mostly been two ways to do this. When these measurements became common, data acquisition equipment was relatively crude. In that case it was common to collect the voltage versus time data from the MFC and output the results on paper using a plotter. The simplest data analysis technique was then to measure the width of the electron distribution at ½ of its peak value, which was known as the full-width-at-half-maximum = FWHM. Thus, some historical data reported beam diameter as: FWHM = 1.66 σ . As data acquisition equipment became more sophisticated it became practical to perform a better analysis of the electron distribution. Thus, in more recent times the beam diameter is often related to the position where the electron density falls to $1/e^2$ of the central value, which is known as the beam full-width-at- $1/e^2$ = FWe-2. In this case beam diameter is: FWe-2 = 2.83 σ . In this paper we will largely discuss the FWe-2 values. As long as the beam is actually Gaussian in shape, both of the common ways to define beam diameter are equivalent in that they both relate to the Gaussian width parameter, σ .

One important point, relative to the FWe-2 values used in this report, should be mentioned. These data result from use of an enhanced MFC, that the vendor has called an EMFC. The software supplied with the EMFC beam profiling device actually yields FWe-2 values that are just the diameter of a circle that encloses 86% of the total beam current with no curve fitting involved in the analysis. For a symmetric Gaussian beam, this simple diameter calculation is identically equal to the actual value that would result from a least-squares curve fit to the data. For more complex beam shape this simple approach could deviate considerably from a more proper curve fit to the data. However, it is important to note that typical data from HVEB machines, such as shown in Figure 1, usually are sufficiently Gaussian and circularly symmetric that a more proper least-squares curve fit and the simple FWe-2 value are effectively identical. Another important point is that the beam can be significantly elliptical and the simple 86% definition still works as long as the beam is overall Gaussian in nature. If the beam is described by superimposed Gaussians, which are described mathematically by an equation of the form:

$$J = J_0 \exp(-r^2 / \sigma_x^2) \exp(-r^2 / \sigma_y^2)$$

then the 86% FWe-2 is just the average value of σ_x and σ_y and is still a reasonable description of the beam. It should be noted that the usefulness of FWe-2 probably fails if the beam is sufficiently elliptical. If the beam is highly elliptical it seems reasonable that it would matter how the beam travel direction is oriented relative to the beam elliptical shape. This matter is the subject of ongoing research but preliminary data suggests that ellipticity values up to perhaps 1.5 are largely irrelevant to the resulting weld dimensions.

There is another way to define beam diameter. This alternative is suggested by an international standard: ISO 11146-1, "Lasers and laser-related equipment – Test methods for laser beam widths, divergence angles and beam propagation ratios – Part1: Stigmatic and simple astigmatic beams". While this standard was adopted to pertain to laser beams, it still provides a reasonable methodology to apply to EB. This standard defines diameter by computing the second moment of the power density distribution. Basically, this is an integral over the total distribution where the local power density is weighted by the square of its distance from the centroid of the distribution. The result of the second moment calculation is herein called D_{2M} . These are the beam diameter values returned by the commercial beam profiler sold by Pro-

Beam, the PBD. Some details of the PBD and its results are contained in: "Evaluation of Two Devices for Electron Beam Profiling", P. Burgardt and S.W. Pierce, LA-UR-14-28680. It is important to note that for a Gaussian beam, D_{2M} and FWe-2 are identical.

At least some of the problems being discussed in this paper may be related to the fact that the two beam diameter values, D_{2M} and FWe-2, can be substantially different under some conditions. For those data shown on Figure 1, $D_{2M} \approx 1.2$ FWe-2. Even though those beam current densities are nearly Gaussian, there are some fraction of the electrons outside of the Gaussian distribution at radii significantly away from the beam center. Those electrons represent a small fraction of the total beam (typically < 10%) and have little effect on the FWe-2 calculation but, since those few electrons are weighted by the square of their radius from the center in the second moment calculation, they will significantly increase D_{2M} . Considering data from a number of different high voltage EB machines it appears that $D_{2M} = 1.1 - 1.4$ FWe-2 is typical. However, even though D_{2M} and FWe-2 are often a bit different in absolute value, their determinations of minimum beam size and the relative change in beam size with focus seem to be consistent for the HVEB machines studied previously. Nevertheless, it is easy to see that the second moment diameter is unusually sensitive to electrons away from the core of the beam and that D_{2M} could be anomalous for a non-Gaussian beam shape.

Typical beam size data for FWe-2 for a HVEB are shown in Figure 2. This plot results from the usual way to collect the data, which is to measure diameter as a function focus coil current. It should be noted that the sharp focus point (about F = 693) on Figure 2 agrees with the sharp focus point determined by the usual manual sharp focus determination.

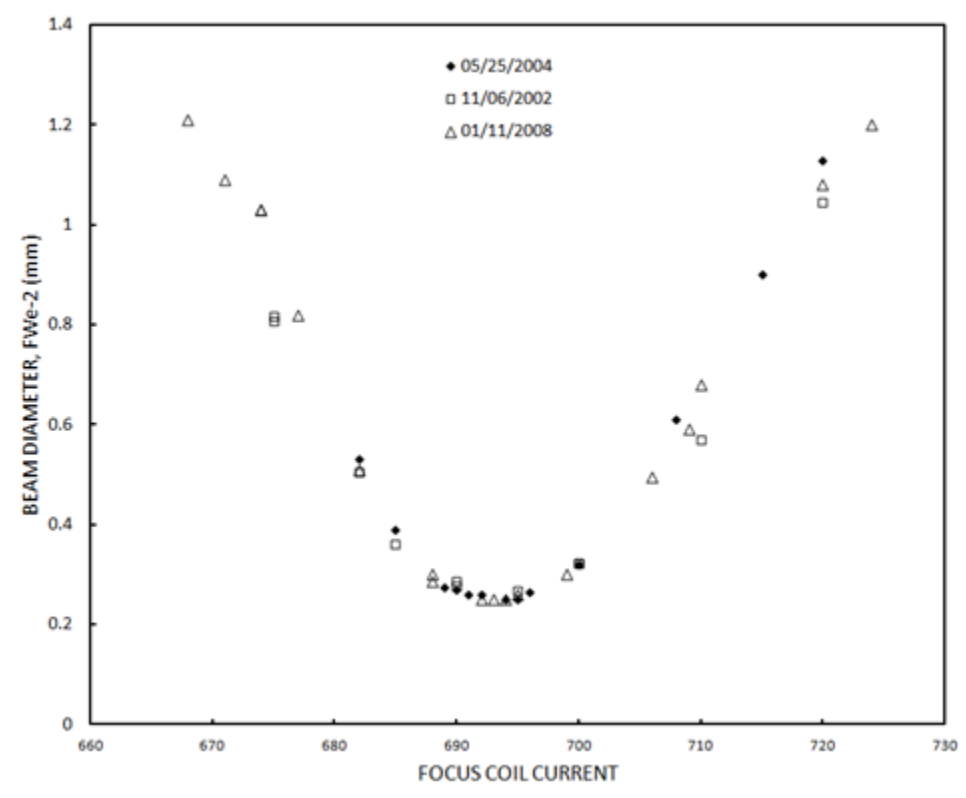


Figure 2: Typical measured FWe-2 versus focus coil current for a HVEB machine (110 kV; 10 mA; 310 mm working distance). These are the beam diameter values used in Figure 3.

Supporting Experimental Data

In order to understand the importance and significance of beam diameter, some supporting historical weld data will be presented. In the past a considerable study of the correlation of FWe-2 (actually, FWHM was used early in this research) with weld behavior was undertaken. Most of the early work involved welds in Type 304 and Type 21-6-9 stainless steels welded with a typical HVEB. The general conclusion from that research was that the weld dimensions correlated nicely with the measured beam size when beam diameter was defined as FWe-2. Figure 3 shows weld pictures that illustrate that point. As can be seen, maximum weld

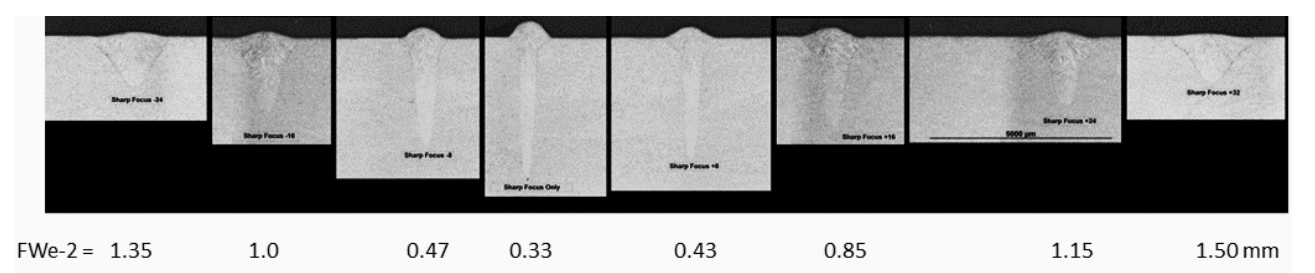


Figure 3: Weld cross-section for welds in Type 304 stainless steel as obtained on a typical high voltage electron beam welding machine (110 kV; 10 mA; 25.4 mm/s travel speed; 310 mm working distance). The weld sections are correlated with the measured beam diameter.

penetration occurs at the minimum beam size and that the weld gets shallower and wider in a predictable fashion as the beam diameter increases. The beam diameter values shown on Figure 3 come from EMFC measured beam diameters, which are shown on Figure 2.

The statement about maximum weld penetration occurring at sharp focus is a bit oversimplified. In reality, maximum weld penetration is known to occur for a bit of underfocus. Considerable historical data suggests that maximum weld penetration actually occurs when the beam minimum size is displaced downward into the keyhole roughly d/2. For welds with d < 8 mm (and the relatively long depth-of-focus of the EB) the difference is insignificant and is comparable to normal experimental uncertainties. All of the data presented herein have sufficiently small penetration that sharp focus is consistent with the minimum beam diameter being located at the material top surface.

Figure 4 is a plot of measured weld depth versus beam diameter from the Figure 2 welds showing that weld penetration is consistent with power-law behavior (the power law behavior and the experimental power law coefficients are consistent with heat flow calculations for a weld with this shape). This general behavior was found to apply to all materials studied with some complicating factors, related to the material thermal properties, which will be discussed later.

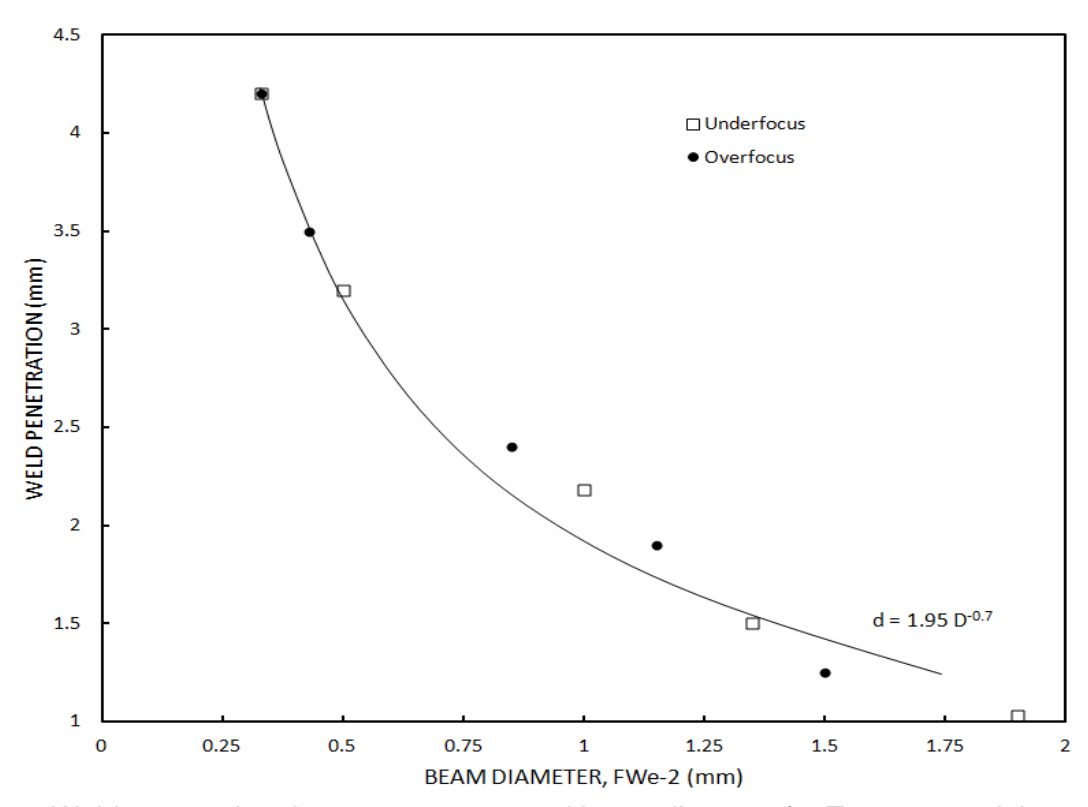


Figure 4: Weld penetration data versus measured beam diameter for Type 304 stainless steel as obtained on a typical HVEB welding machine (110 kV; 10 mA; 60 ipm travel speed; 310 mm working distance – the welds in Figure 2). The solid curve is a typical power law fit to the data.

Another way to consider the validity of the FWe-2 definition of beam diameter is that it should also correlate with the width of the weld. When in the deep penetration mode of welding (weld depth to width ratio, d/w > 2) and at reasonably high travel speed (typically greater than about 40 mm/s), the width of the weld (when properly defined) should be directly related to the beam diameter because the keyhole opens up only under the high power density portion of the beam. Figure 5 illustrates the appropriate weld width to consider in this analysis, W1/2. When weld width is defined in this way, there is a direct relationship between weld width and the measured beam diameter. Figure 6 illustrates that point. As can be seen, beam diameter defined as FWe-2 does correlate with weld width. There are two details important to this discussion. First, the correlation of W1/2 with FWe-2 only works well for deep penetration welds with d/w > 2 (and the correlation actually works fairly well down to $d/w \approx 1$). This is because once the heat flow becomes more 3D in nature, the weld shape becomes nearly independent of the heat source size and depends mostly on other factors such as convection in the weld pool. The other point is that the W1/2 versus FWe-2 plot has a non-zero intercept because there is always some melting of metal outside of the keyhole. That non-zero intercept value is travel speed dependent and becomes nearly zero for v > 40 mm/s.

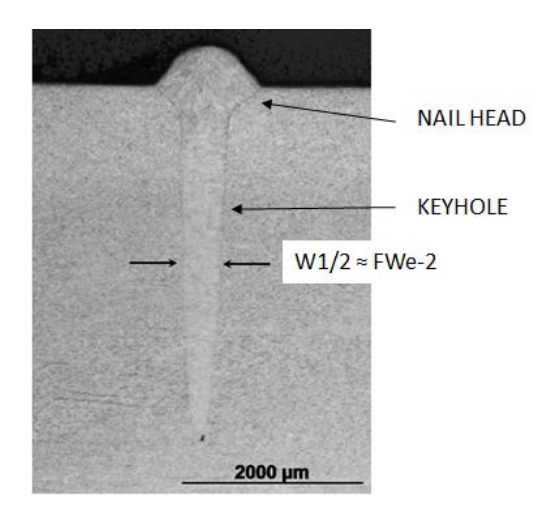


Figure 5: Example of the W1/2 measurement and its relationship to the actual beam size. This weld is the sharp focus weld in stainless steel from Figure 3 (110 kV; 10 mA; 25.4 mm/s travel speed; 310 mm working distance).

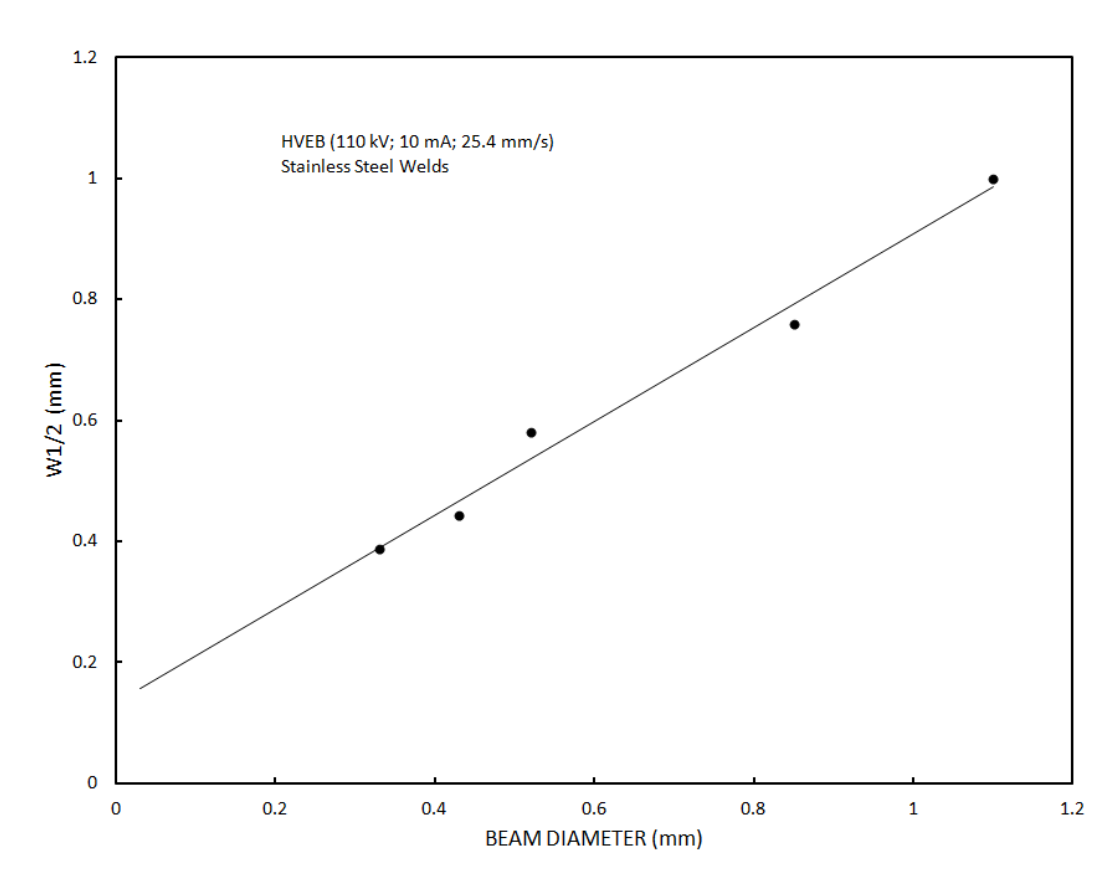


Figure 6: W1/2 values versus measured beam diameter (FWe-2) for Type 304 stainless steel as obtained on a typical HVEB welding machine. These data are measurements from the data shown in Figure 2.

The essential point is that FWe-2 seems to be an entirely satisfactory definition of beam diameter for stainless steel at least for this style of high voltage EB machines. Additionally, D_{2M} is probably an equally good diameter measurement for a simple beam shape since it is the same within a multiplicative constant (this assertion is the subject of ongoing research and is actually conjecture at this time).

Up to this point the discussion has only involved stainless steel welds and it is reasonable to ask to what extent FWe-2 works for other materials. The early extensive research on this subject (by Burgardt circa 1985, unpublished results) showed that this beam diameter works fairly well for a wide range of materials. Figure 7 shows weld penetration data versus beam size for four

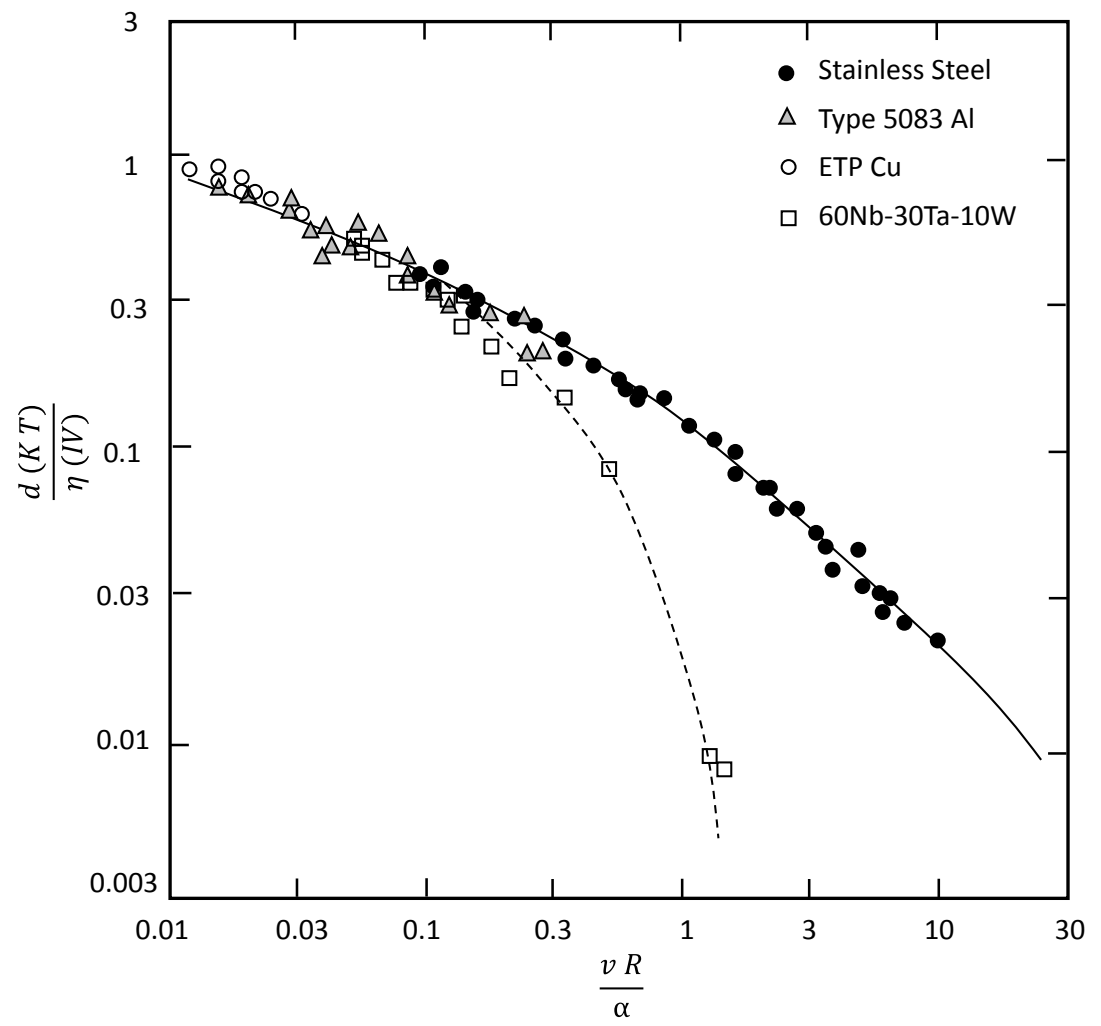


Figure 7: Universal plot of weld penetration versus dimensionless beam size for a number of materials welded in deep penetration mode. This demonstrates that the same definition of beam size applies to a variety of materials.

considerably different materials (two stainless steel alloys, an aluminum alloy – 5083, nominally pure copper and a Nb-Ta-W alloy known as Fansteel85) and shows that they all behave similarly using this beam diameter definition. That research showed that maximum penetration occurs at sharp focus and that weld depth correlates with FWe-2 similarly for all the materials studied.

Figure 7 does make use of unusual variables, which do require a bit of explanation. The particular variables plotted on Figure 7 are dimensionless quantities suggested by a fundamental study of heat flow around a weldment with a large d/w ratio (the data all represent cases with d/w > 2). The vertical axis is dimensionless weld penetration where: d is measured weld depth; η IV is power input for the particular weld (η , the process efficiency was assumed constant = 0.9); κ is the material thermal conductivity; T is the keyhole wall temperature (about 0.8 Tb, the boiling point). The horizontal axis is dimensionless beam size: v is travel speed; R is measured beam radius (FWe-2 / 2); α is the material thermal diffusivity. An important additional detail is that the data follow theoretical expectations when the temperature dependent material properties are assumed constant at values midway between the melting point and room temperature. The solid curve drawn on the figure is a theoretical curve that represents dimensionless penetration versus dimensionless beam size that should result for deep penetration welds.

The basic reason we show Figure 7 is that it illustrates the overall validity of the usual beam diameter definition for materials with a wide range of thermal properties. There are some deviations from the theory when the data are considered in detail, but overall, weld penetration was nicely consistent with theoretical expectations for deep penetration welds in all of the materials studied. This strongly suggests that the FWe-2 definition of beam diameter is valid over a wide range of machine variables and material conditions. Interestingly, the best fit of the experimental data to theory actually occurred when beam diameter was assumed to be roughly midway between the measured FWe-2 and D_{2M} values for that particular machine. Of course, it is not apparent that any of this would pertain to a non-Gaussian beam shape especially in regard to the equivalence of FWe-2 and D_{2M} .

Another important concept illustrated on Figure 7 is the dashed line drawn on the Fansteel85 data. The Fansteel85 (FS85) welds were made in support of a particular production application so were all made at a fairly modest beam power of 700 - 1000 W. With that moderate power input, deep penetration welds resulted over only a limited range of (vR/α) near to sharp focus. Increasing (vR/α) resulted in a quick change from keyhole welds to conduction mode welds with $d/w \approx 0.5$ (welds largely independent of beam size) and even further increases in (vR/α) resulted in no melting at all. That is the origin of the dashed line deviating from the theoretical curve and then rapidly plunging towards zero penetration at about $(vR/\alpha) = 2$. These experimental results can be correlated to beam power density, which for this refractory alloy corresponds to about: keyhole formation requires P' > 6000 W/ mm² and no melting occurs for P' < 1000 W/ mm². The corresponding values for stainless steel are about a factor of 4X lower than this. The essential concept is that a material with reasonably large thermal diffusivity and high melting point will seem to have somewhat unusual weld behavior because regions of the beam with a power density high enough to contribute to keyhole formation in stainless steel would not do so in the refractory alloy. Since the Fansteel85 properties are similar to the Ta-10W properties, a similar response is expected for the Ta-10W material of importance to this report. The point is that beam diameter, FWe-2, is a good description of the overall beam size, which does adequately represent the overall weld behavior, but that the material response to changes in beam size can be complex for the refractory alloy.

Further corroborating evidence for this conclusion about the refractory alloy is contained in Figure 8. Here we see weld shapes that resulted from sharp focus welds in a number of

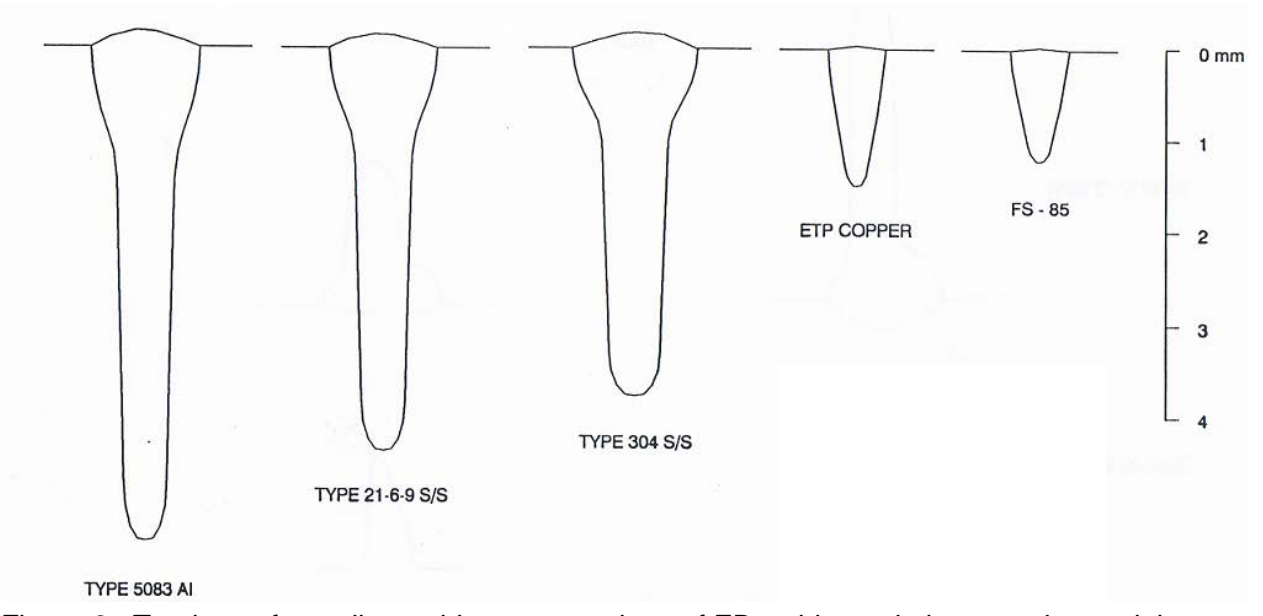


Figure 8: Tracings of metallographic cross-sections of EB welds made in several materials at the same welding variables. These welds were all made with weld variables: HV = 100 kV; BC = 7 mA; V = 12.7 mm/s; sharp focus (FWe-2 = 0.25 mm). This illustrates the wide variation in weld shape that results from different material thermal properties.

different materials made at sharp focus with a modest beam power of 700 W. In many materials the deep penetration welds exhibit a keyhole portion of the weld along with a noticeable nailhead; this is illustrated in Figure 5. As can be seen in Figure 7, the FS85 welds had no discernable nailhead. Further, the W1/2 values for the FS85 welds were comparable to but noticeably smaller than those seen in the stainless steels and the aluminum alloy. This suggests that the details of power density in the beam are relevant to the weld result.

In order to illustrate the importance of power density to the welds, consider Figure 9 (which is a copy of the sharp focus data shown in Figure 1). It should be stated immediately that the conclusions we present in relation to Figure 8 are not supported by rigorous heat flow calculations but do make sense relative to observed weld behavior. On Figure 9 we have drawn arrows that illustrate the radii of the beam that correspond to particular power density locations for the FS-85 refractory alloy. The first arrow is labeled as "keyhole". Its significance is that inside of that beam diameter the beam power density is large enough to produce a keyhole (P' > 6000 W/ mm²). The other arrow is labeled "no melting". Its significance is that outside of that beam diameter the beam power density is too low to produce melting (P' < 1000 W/ mm²). Interestingly in this particular case, the "no melting" arrow happens to be essentially equal to FWe-2 for that beam. Thus, it is reasonable that the welds in FS-85 would have a keyhole a bit narrower than FWe-2. The lack of a nailhead is also probably consistent with this overall picture. In a material like stainless steel, the power density required for melting encompasses most of the electrons detected in the wings of the Gaussian distribution (ie. a significant number of electrons at a distance from the beam core greater than the diameter defined by FWe-2). . In this example power that can contribute to melting in stainless steel extend out to a diameter

of at least 0.8 mm, which is consistent with the result shown in Figure 8. The FS-85 welds show no significant nailhead because the cutoff for melting is inside the overall Gaussian distribution and the beam power in the wings of the beam power distribution cannot contribute to melting. It is also interesting to note that the weld behavior in Cu was similar to that of the FS-85. That is so because the onset of melting and keyhole formation happen when P' becomes greater than a value related to κT (where, κ is the material thermal conductivity and T is the melting and boiling points respectively). Therefore, a relatively high sensitivity to beam power density occurs in materials with high thermal conductivity and/or high melting temperature. The essential point to this discussion is that actual weld behavior is a result of the interaction of the beam power density with the material thermal properties.

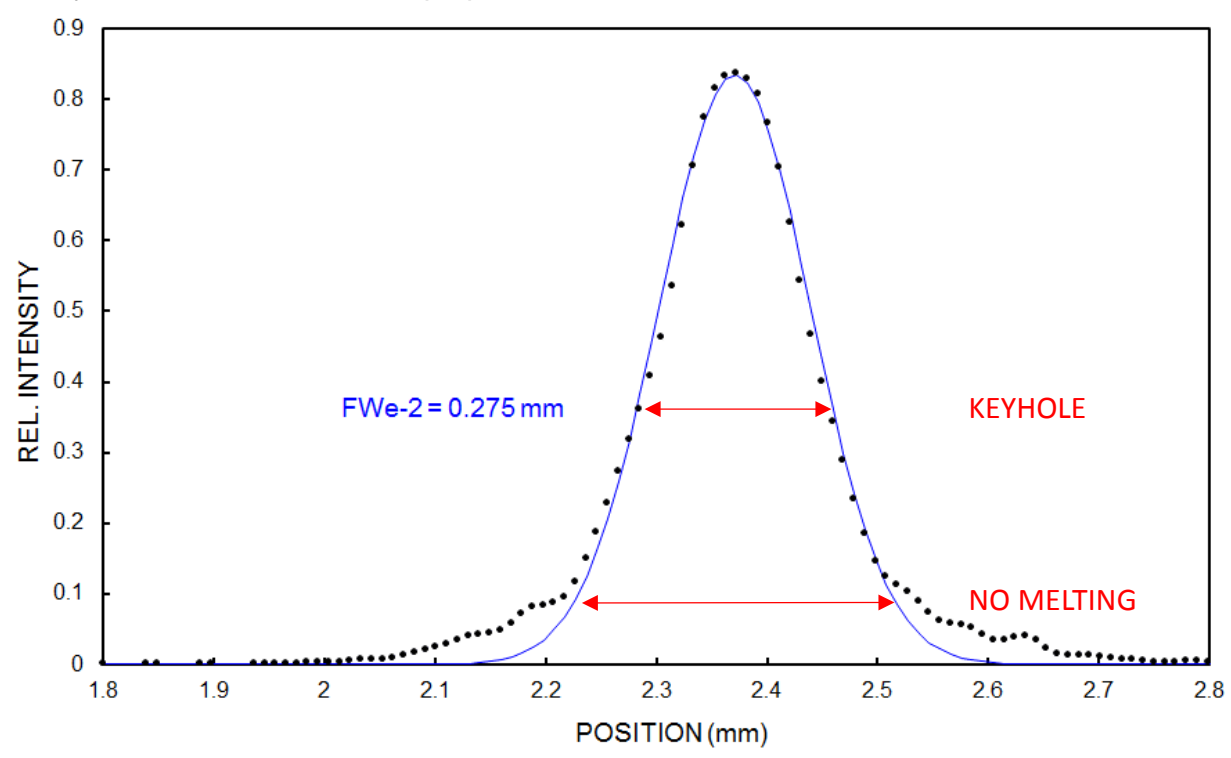


Figure 9: Beam power density versus radial position for a typical HVEB. The red arrows indicate the radii of the portions of the beam where the power density is relevant to keyhole formation and where the power density becomes too low to contribute to melting for the FS-85 refractory alloy.

All of the basic research on the subject of beam diameter has led to the conclusion that a simple definition of beam size such as FWe-2 or D_{2M} is an adequate indicator of the electron beam size with the weld dimensions correlating well with that beam diameter definition. Weld penetration behavior in EB welding can appear to deviate significantly from agreement with beam diameter because of the interaction of beam power density with the material thermal properties (especially true for materials with high thermal conductivity and/or melting point). However, this isn't necessarily an indication that the beam diameter definition is faulty; it is simply that the material can react to that beam size in a complex way. Nevertheless, the historical data do suggest that the most useful definition of beam diameter might be more indicative of the power density distribution in the beam.

RESULTS AND DISCUSSION -LOW VOLTAGE EB MACHINE

The specific problem actually being addressed in this paper is related to a particular production weld development project involving a Ta-10W alloy. This weld is to be made with a low voltage electron beam (LVEB) machine presently installed at LANL in Building SM-39. Some details about that machine are contained in: "Characterization of Pro-Beam Low Voltage Electron Beam Welding Machine", S.W. Pierce and P. Burgardt, LA-UR-15-21173 (2015).

A number of welds in the Ta-10W alloy as well as some supporting welds made in Type 304 stainless steel were made with the LVEB. All welding techniques and weld evaluation methods were standard for this sort of development work. Initial screening experiments showed that quality welds (beam broadened a bit by defocus and/or beam oscillation) with the required penetration would require the basic parameters: HV = 60 kV; BC = 60 mA; TS = 60 ipm = 25.4 mm/s; work height = 100 mm. Therefore, all data unless otherwise noted were collected at that basic starting point. Accompanying the welds, considerable beam profiling data were obtained with the PBD profiling device, which is described in some detail in: "Evaluation of Two Devices for Electron Beam Profiling", P. Burgardt and S.W. Pierce, LA-UR-14-28680 (2014). Do note that the PBD software yields beam diameter values of D_{2M} , which may contribute to the focus discrepancy that will be discussed subsequently.

Typical Beam Profiling Data - LVEB

Prior to the welding work, the beam was thoroughly characterized with the PBD diagnostic device at the required beam parameters. An example of the resulting beam profiling results is shown in Figure 10. As can be seen, the beam profile data seem to be of high quality and show that the minimum beam size (sharp focus) occurs at a focus current of about 1910 based on a simple examination of the diameter values from the PBD looking for the smallest value.

Figure 10 illustrates that there is some ambiguity in how one chooses the sharp focus beam size. There is typically some scatter in the data near to sharp focus and, therefore, some sort of curve fit to the data may be useful. The curve through the data in Figure 10 is a typical least squares hyperbolic fit to the data, which should theoretically describe the beam diameter. The curve fit illustrates that the minimum measured beam size and a curve fit won't necessarily yield the same result. The fit assumes that the data is represented by a function of the form: $D^2 = C \ (\Delta F)^2 + (Min)^2 \ , \text{ where D is the experimental diameter value } (D_{2M}); C \text{ is a "best fit" constant, called slope on the figure; } \Delta F = F - F_C \ ; F \text{ is the experimental focus value; } F_C \text{ is the centroid value of focus } (\text{the "best fit" sharp focus point); } (Min) \text{ is the appropriate "best fit" minimum beam diameter. This curve fit indicates that the proper sharp focus value is <math>F = 1912$ while the smallest experimental beam size value is at F = 1910. Multiple measurements of sharp focus, using the curve fit technique, showed that sharp focus for these conditions is: 1914 + 7 - 3 mA.

It is also worth mentioning that the interesting deviation of the measured beam size data from the theoretical curve fit around sharp focus is common in those data. As will be discussed later in this paper, that interesting behavior around sharp probably indicates that the beam power density versus focus has a complex behavior for this particular machine. That may be related to the sharp focus discrepancy that is the main topic of this paper.

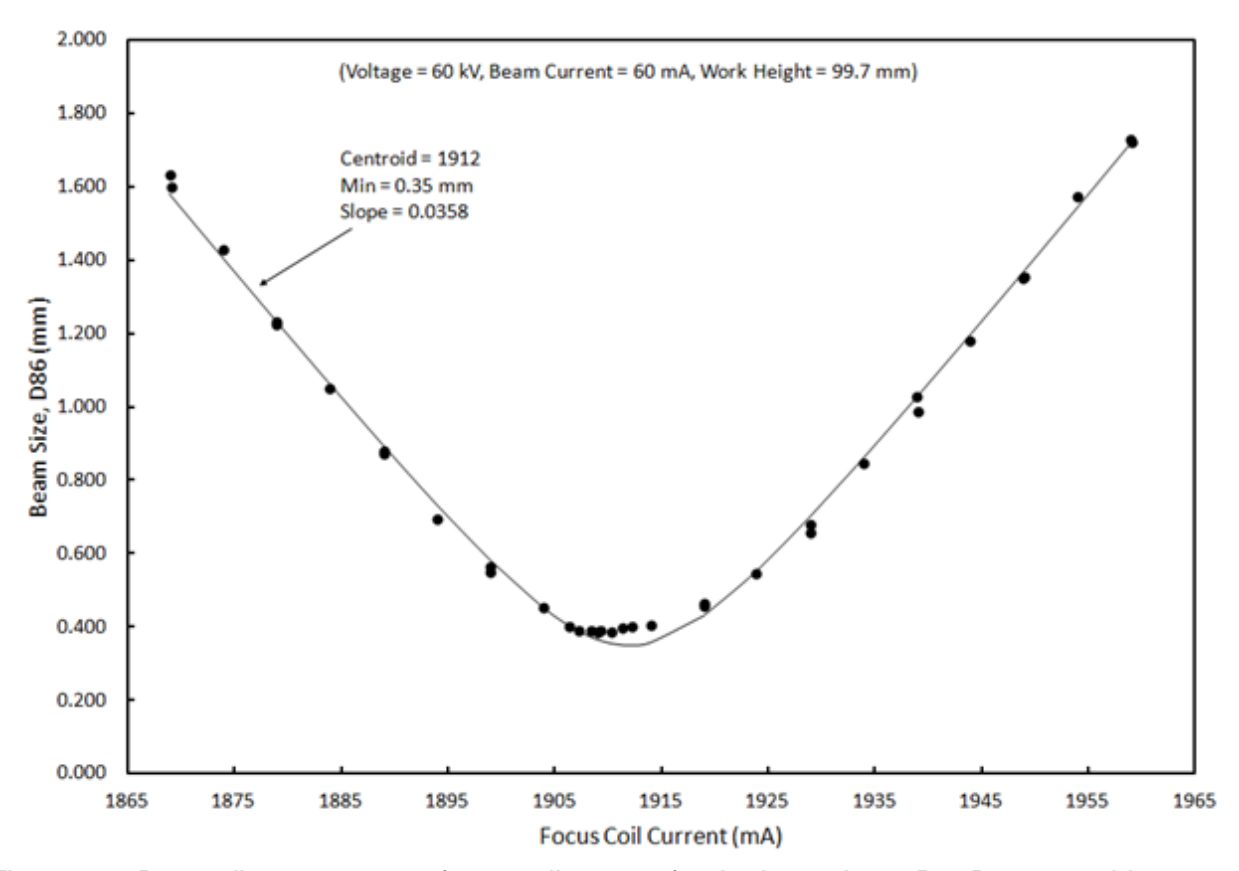


Figure 10: Beam diameter versus focus coil current for the low voltage Pro-Beam machine installed in SM-39. These data were obtained with beam parameters: high voltage = 60kV; beam current = 60 mA; work height = 100 mm.

Comparing Figure 2 data with Figure 10 beam diameter data we conclude that the welding behavior of the LVEB should be essentially identical to what has been seen on the usual HVEB machines. Maximum weld penetration should occur at the minimum beam size (with the caveat that the beam size seems to increase little for modest defocus away from sharp focus on this particular LVEB, which may confuse those results a bit) and the change in weld width and penetration for a given amount of defocus should be comparable for the HVEB and LVEB machines.

Weld Penetration Data - Ta10W Alloy

The first indication that there was a problem with the beam diameter definition as applied to this LVEB came during the initial welding phase of this project. Those initial welds are illustrated in Figure 11. As can be seen on Figure 11, the measured sharp focus point was about F = 1912 mA but that maximum weld penetration in the Ta-10W material occurred at about F = 1930 mA. Further, looking at the weld generated at F = 1910 makes it clear that the beam seemed to be significantly defocused at the measured sharp focus point. Note that the beam diameter values shown in Figure 11 are values of D_{2M} determined by the Pro-Beam beam diagnostic tool (PBD).

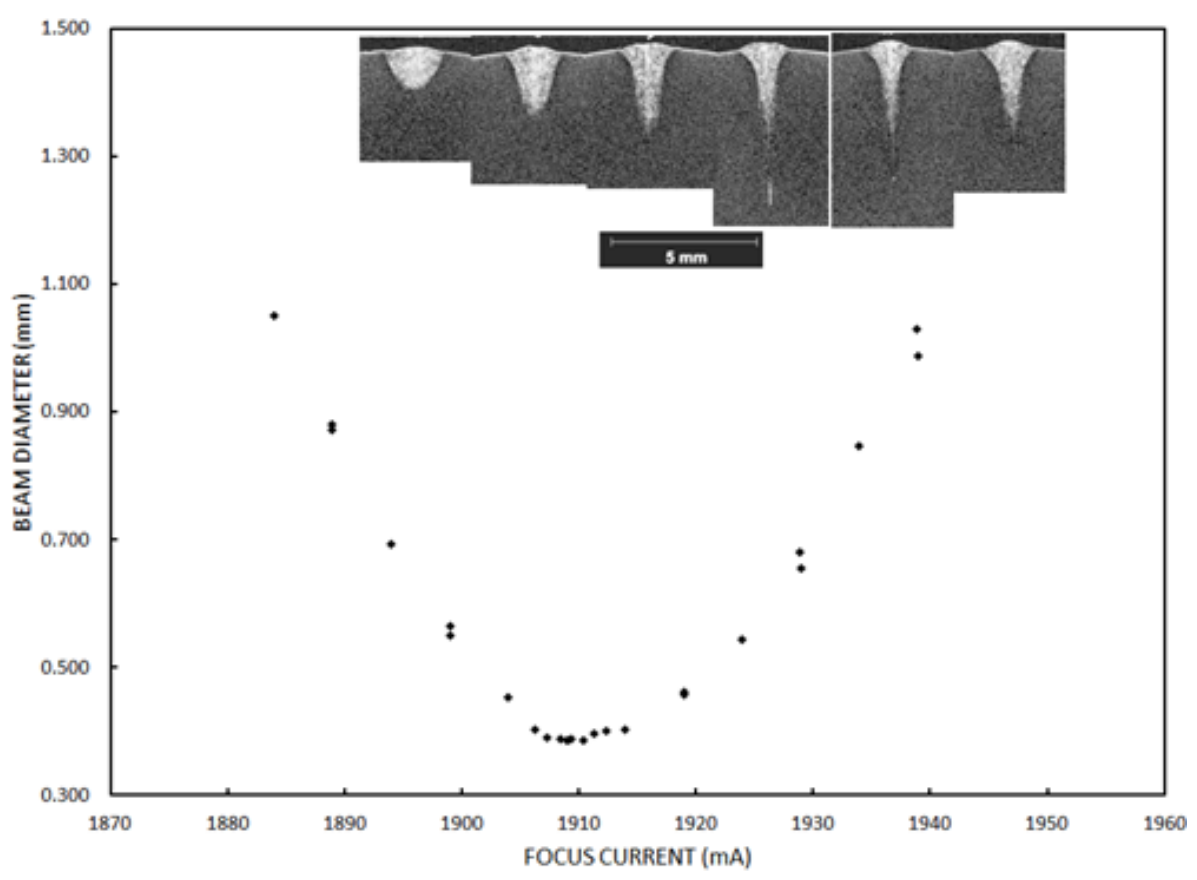


Figure 11: Beam diameter versus focus coil current with accompanying weld cross-sections for the Ta-10W alloy. These data are for the LVEB with beam parameters: HV = 60kV; BC = 60 mA; work height = 100 mm.

Considerable additional welding in the refractory material ensued to eliminate the possibility that the focus discrepancy was simply experimental error. This additional welding was driven largely by our experience that the determination of beam sharp focus was considerably variable at the time of those initial weld development activities. We believe that this variability was eventually traced to chamber pressure effects. During those initial weld development activities the chamber vacuum was considerably variable due to problems with the vacuum pump and vacuum gauge. It is known that chamber pressure does affect sharp focus and overall beam size. After that, machine maintenance was performed and we were more careful about maintaining a constant chamber pressure; the sharp focus variability was minimized and now seems to be at an acceptable level.

Additional welding experiments were subsequently carried out on the Ta-10W material and those results are summarized in Figure 12. As can be seen there was once again a considerable difference between the measured sharp focus point, F = 1917, and the focus value for maximum weld penetration, at about F = 1928. One can also see in Figure 12 that the focus discrepancy of about 11 mA is quite significant to the weld dimensions that result in this weld. Some further corroborating data was generated in a nominally pure Ta specimen (this experiment being performed largely to test the possibility that there was something really unique about the Ta10W alloy). A longitudinal section of a weld in the Ta specimen generated with a "sloped" focus coil current is shown in Figure 13. The important point is that the Ta experiment shows similar behavior to the Ta-10W results with the weld penetration changing little over a rather wide range of focus but that the maximum penetration was at about F = 1929. All of this additional weld development work confirmed that there was a repeatable and significant discrepancy between the measured weld penetration and the beam profiling data when applied to the Ta-10W alloy.

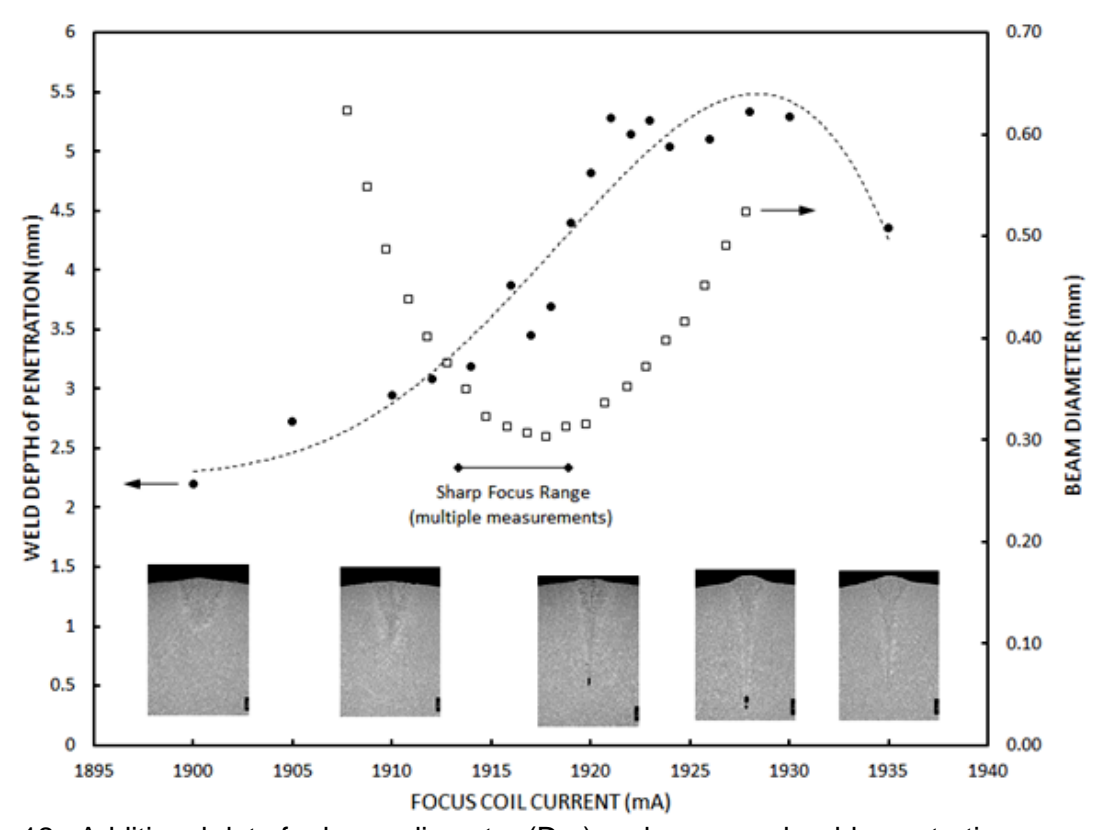


Figure 12: Additional data for beam diameter (D_{2M}) and measured weld penetration versus focus coil current with accompanying weld cross-sections for the Ta-10W alloy. These data are for the LVEB with beam parameters: HV = 60kV; BC = 60 mA; work height = 100 mm.

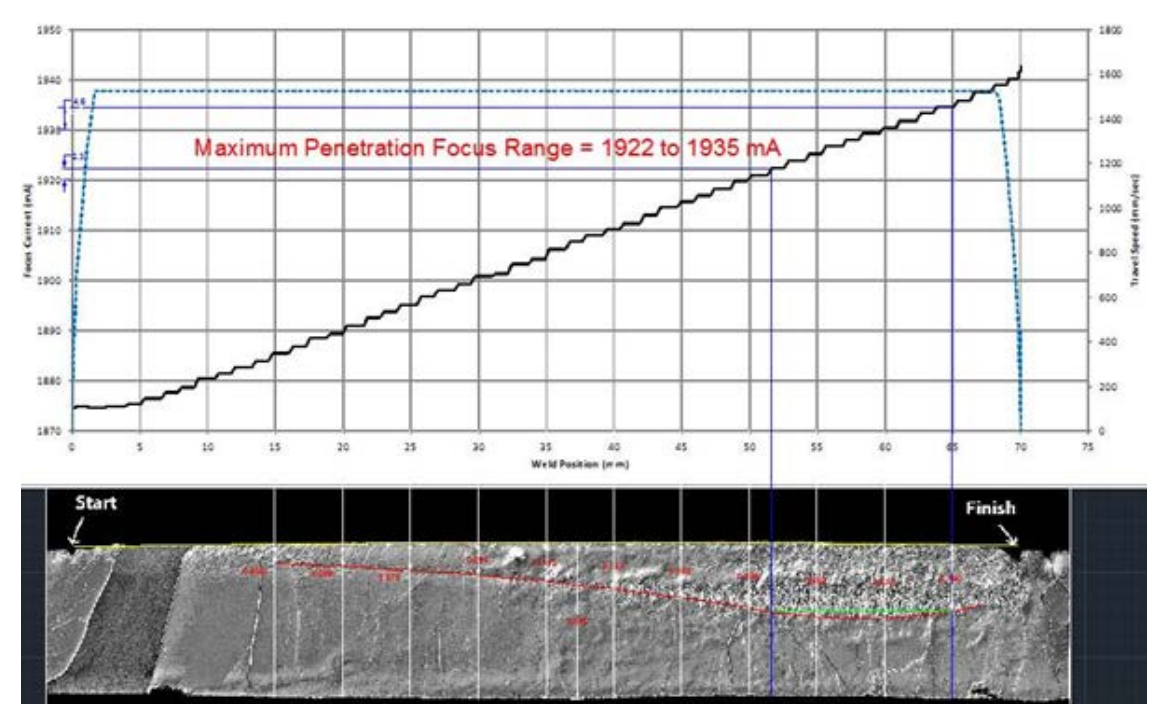


Figure 13: Longitudinal metallographic section of a weld made in Ta along with a graph showing the focus coil current correlated with position on the met section. These data were obtained at the usual beam parameters but with sloping focus coil current.

Additional Supporting Data - Welds in Stainless Steel

Since there is at least some possibility that the sharp focus discrepancy could be related to some special property of the Ta-10W alloy, some supporting weld data were obtained on stainless steel. Type 304 stainless steel was chosen for this work because it is well-established that weld behavior in this material correlates well with beam profiling at least for the HVEB machines. If sharp focus issues persist in this material, we can be certain that there is some problem peculiar to the ProBeam LVEB.

The welding experiment was carried out at the usual welding parameters (60 kV; 25.4 mm/s; 100 mm work height) but at two different beam current levels. The first set of welds was made at a beam current of 20 mA and the resulting weld cross-sections are shown in Figure 14. The weld cross-sections are arranged according to the focus coil current used to make the welds. Accompanying the pictures are the corresponding beam diameter values (D_{2M}); for each focus value. As can be seen, weld penetration generally corresponds to the beam diameter with maximum penetration occurring at the PBD determined sharp focus value, within experimental error. In other words, these data basically agree with our expectations about weld behavior versus beam diameter.

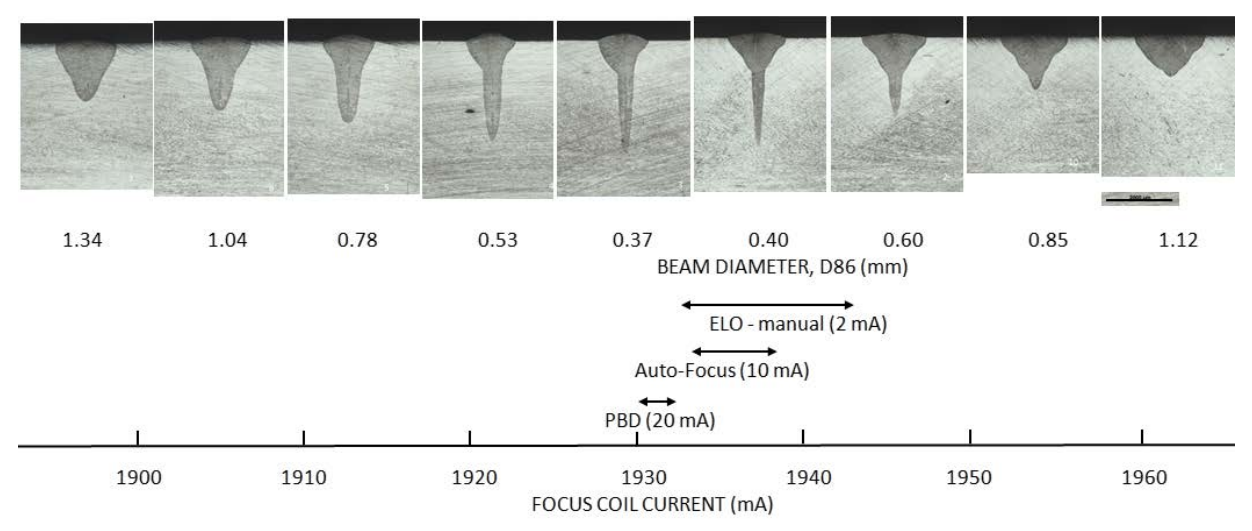


Figure 14: Cross-sections of welds made in stainless steel at the usual weld variables (60 kV; 25.4 mm/s; 100 mm work height) and with a beam current of 20 mA. The horizontal arrows indicate the range of sharp focus determined by three methods.

On Figure 14 we have also indicated the measured sharp focus location; this requires a bit of explanation. There are three ways that sharp focus may be determined on the ProBeam machine. The first two methods look for the sharpest image in the backscattered electron picture of the workpiece and its surroundings. The first is called ELO-manual. This consists of using a low power beam (2 mA beam current in this case) and the operator manually adjust focus to look for the sharpest image (basically equivalent to the usual operator manual focus on a tungsten block). The second method is called auto-adjust or auto-focus. In this case a bit higher beam power is used (10 mA beam current is typical) and the machine automatically finds the sharpest image using image analysis software. The final sharp focus determination used here uses the PBD device to measure the beam profile over a range of focus values and the minimum beam size is identified. This measurement is done at full beam power. Those results appear on the figure as "PBD". Looking at Figure 11 one can see that the resulting sharp focus determinations are significantly different. Part of the difference undoubtedly happens because they are different measurement techniques and may yield a bit different results. However, most of the difference in sharp values is because of the shift downward in sharp focus that occurs with increasing beam current. That was seen and reported in: P. Burgardt and S.W. Pierce, "Characterization of Pro-Beam Low Voltage Electron Beam Welding Machine", op. cit. The sharp focus information is presented to point out that a proper and consistent method for sharp focus determination on this machine is critical and that there are multiple ways to do that which will yield different results.

A second welding experiment was carried out in the Type 304 stainless steel. The welds were made at the usual welding parameters (60 kV; 25.4 mm/s; 100 mm work height) but with a beam current of 40 mA. The resulting weld cross-sections are shown in Figure 15 along with the sharp focus values obtained at that time. Once again we see that weld penetration generally corresponds to the beam diameter with maximum penetration occurring at the PBD

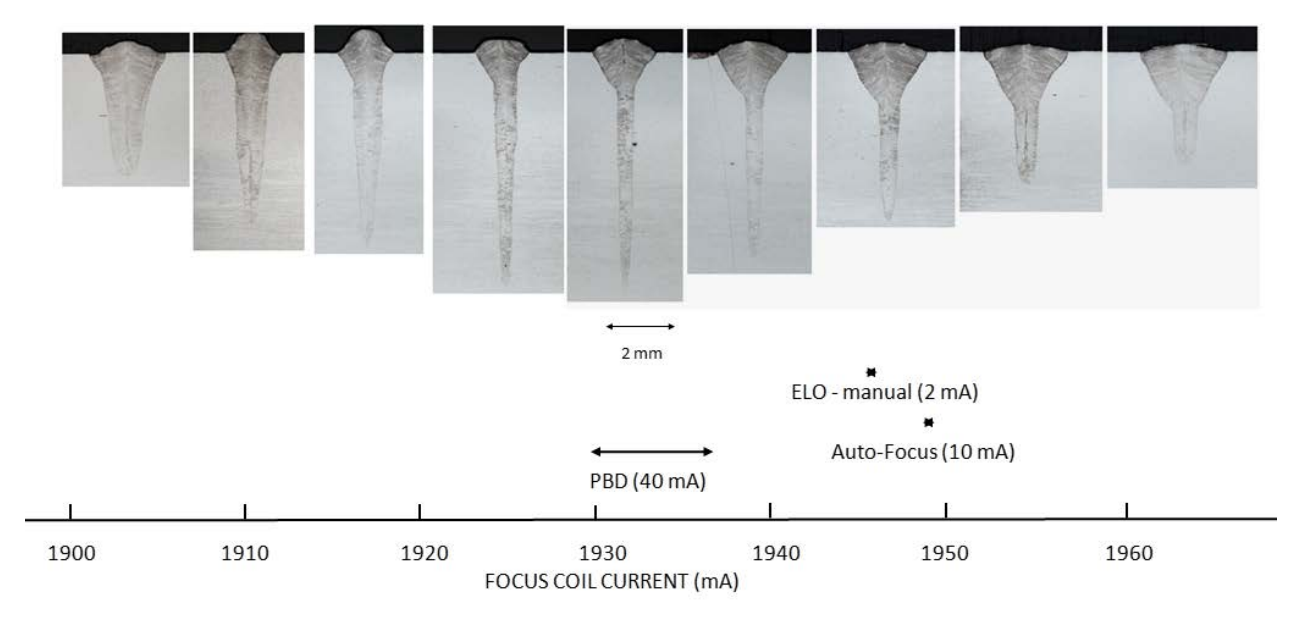


Figure 15: Cross-sections of welds made in stainless steel at the usual weld variables (60 kV; 25.4 mm/s; 100 mm work height) and with a beam current of 40 mA. The horizontal arrows/symbols indicate the range of sharp focus determined by three methods.

determined sharp focus value. Looking closely one can see that there is an interestingly large variation in PBD sharp focus and that the Auto-focus and manual focus values are considerably different than was seen previously. This does reinforce the point that sharp focus determination on this machine is technique dependent. The important point is that welds in stainless steel do generally agree with expectations relative to weld penetration versus beam diameter. This seems to suggest that the sharp focus discrepancy seen in the Ta-10W welds is at least partially a result of this material's known sensitivity to beam power density.

Further Analysis of Welds

The sharp focus discrepancy, especially evident in the Ta-10W welds, and the unusual shape of the welds (especially evident in the stainless steel welds) does suggest that there is a peculiarity in the ProBeam LVEB that is contributing to the problem. As we will see, this is apparently related to the details of beam shape on this LVEB machine that result from its particular electron gun design.

The first bit of additional weld analysis performed here is to generate the usual plot of weld penetration versus beam diameter for the stainless steel welds. That result is shown in Figure 16. Overall the weld penetration does change with beam diameter in the expected manner. It is interesting to note that the overfocus welds made at 1200 W power on the LVEB are essentially the same as those made at 1100 W with the HVEB. This suggests that the usual definitions of beam diameter are basically valid for both machines. However, there is a considerable difference in weld penetration for overfocus and underfocus beam for welds made with the ProBeam LVEB that does get more pronounced with increasing beam current. We do have data showing that the beam shape changes considerably passing through sharp focus. In fact, this phenomenon occurs on all EB machines. However, these data strongly suggest that the details of beam shape are unusually important on this LVEB machine.

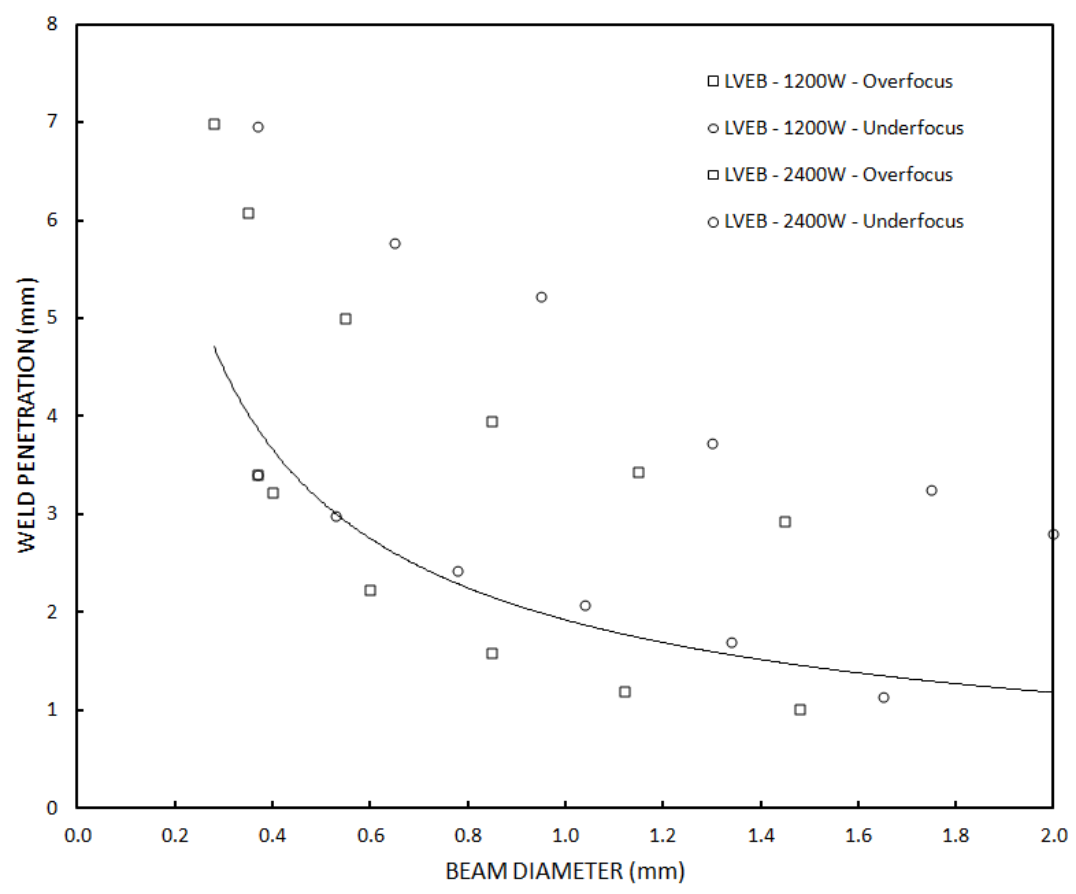


Figure 16: Measured weld penetration versus beam diameter (D_{2M}) for the stainless steel welds made with the ProBeam LVEB. The solid line on the figure describes equivalent welds made with a HVEB at 1100 W of beam power.

Another important clue as to what is probably complicating the ProBeam LVEB results is provided by the resulting weld shape that is especially evident in the stainless steel welds. An example of the unusual weld shape is shown in Figure 17. Here we show an expanded view of

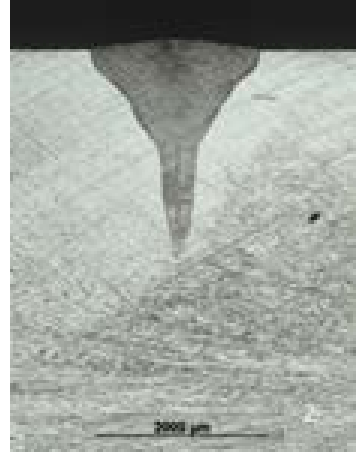


Figure 17: Expanded view of the +20 defocus weld in stainless steel generated at 20 mA with this LVEB machine.

the +20 defocus weld in stainless steel made at beam current of 20 mA. For this weld the beam profiling result was $D_{2M} = 0.6 - 0.7$ mm. However, looking at the shape of that weld it is clear that the beam shape is complex. The "nailhead" portion of the weld appears to be created by some portion of the beam with a fairly large diameter (comparing to the welds shown in Figure 3 leads to the conclusion that some fraction of the electrons have an effective diameter of $D_{2M} > 1$ mm). The most intriguing aspect of the Figure 17 weld is that the keyhole is quite narrow, probably corresponding to a beam width of $D_{2M} \approx 0.3$ mm. In other words, it is clear that the beam consists of two populations of electrons; one population is relatively diffuse and the other is quite narrow. That basic picture accounts for the observed complexities relative to focus.

Some additional information on this effect is revealed by looking more closely at the narrow "keyhole" portion of the welds. As was discussed previously, W1/2 is a measure of the effective beam size creating the keyhole. W1/2 values for the keyhole were measured as best as possible from the welds shown in Figures 12 – 15; those results are summarized in Figure 18. The essential point shown in Figure 18 is that there seems to be a portion of the beam with $D_{2M} \approx 0.3$ mm (ie. the highest power density portion of the beam) that passes through its minimum size at a focus coil current well above the PBD determined sharp focus point. Also, Figure 18 makes it apparent that the difference between the D_{2M} minimum and the focus yielding maximum power density increases with beam current (that is why this effect is most evident in the Ta-10W welds made at 60 mA, where high power density is required).

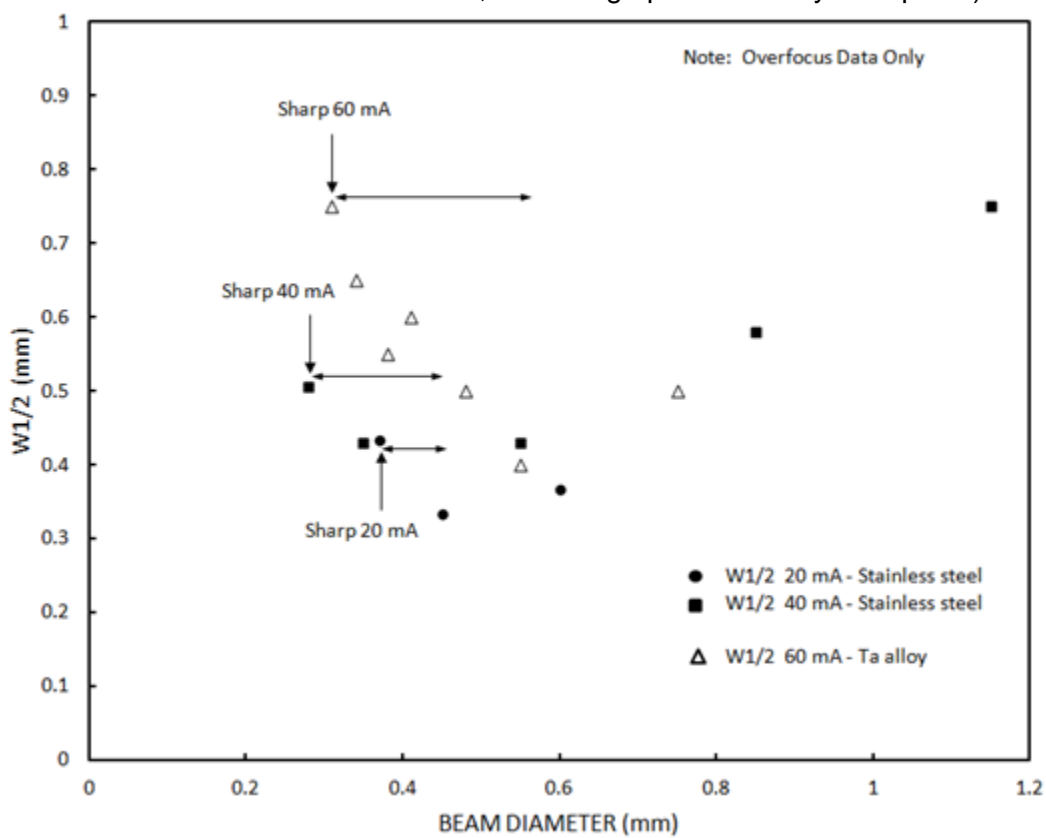


Figure 18: W1/2 values for the stainless steel and Ta-10W welds versus beam diameter (D_{2M}). The horizontal arrows show the apparent shift between the PBD determined sharp focus point and the point of minimum keyhole width.

<u>Detailed Analysis of PBD Data – BEAM SHAPE</u>

The weld data generated with this ProBeam LVEB make it clear that the electron beam of this machine is complex. Therefore, some additional analysis of the beam profiling data from the PBD device is warranted. Specifically, we are looking for direct evidence that the beam from this machine does consist of two populations of electrons (one diffuse and the other quite narrow) that pass through their respective minima at different heights in the beam.

The first piece of this additional analysis is related to the beam shape change at sharp focus apparent in the Figure 16 data. Beam shape change upon passing through sharp focus occurs in all EB machines. In the case of the typical HVEB machines, the beam shape changes a bit when passing through its minimum diameter but that the beam shape changes relatively little when viewed qualitatively. That is why the underfocus and overfocus weld data are generally similar on those HVEB machines. However, for this LVEB there is a substantial difference in the basic shape of the beam for underfocus and overfocus conditions. This point is illustrated in Figure 19. It is quite clear that the beam shape changes fundamentally when passing through sharp focus. Thus, it is understandable that welding behavior for the LVEB would be different for the overfocus and underfocus beam.

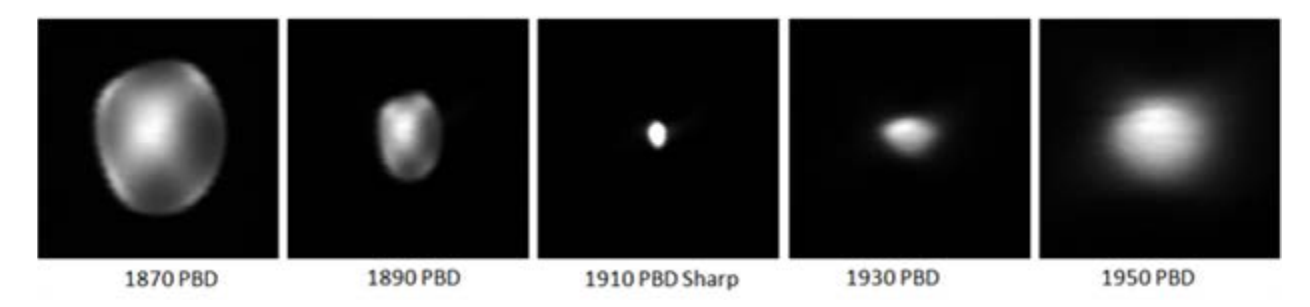


Figure 19: Contour plot of the beam current density for the LVEB at the usual beam parameters. These data illustrate the beam shape change as the beam passes through its minimum dimension.

At this point a brief explanation for the beam shape change as the beam passes through sharp focus is appropriate. In the underfocus beam situation, the beam profiler is looking directly at an image of the electron source (the filament and whatever perturbations are placed on the electrons by the gun design). As focus is changed one is simply looking at the electron source at different magnifications. After the beam passes through sharp focus, the beam shape changes considerably. This happens because the strong space-charge interactions (electrostatic repulsion) between electrons, and especially between electrons with locally high electron density (such as the sharply defined halo electrons in the LVEB), tend to randomize electron trajectories on the local scale when near to sharp focus. The electric field internal to the beam electrons is a conservative field so that the overall convergence/divergence angle of the beam is unchanged but any fine structure in the beam tends to disappear and the details of beam shape will change considerably at sharp focus.

The most important aspect of this re-analysis of the beam profiling results is to look for evidence that the beam does consist of two populations of electrons; one population being relatively diffuse and the other being quite narrow and with high power density. In fact, the data do show this behavior. Figure 20 shows beam profiling (electron density versus position) for an underfocus beam condition. These data were retrieved from the PBD output. As can be seen, at this focus condition the beam does consist of an outer ring of electrons, herein called the "halo", with a high electron density center, herein called the "core". That is certainly consistent with the weld behavior noted previously.

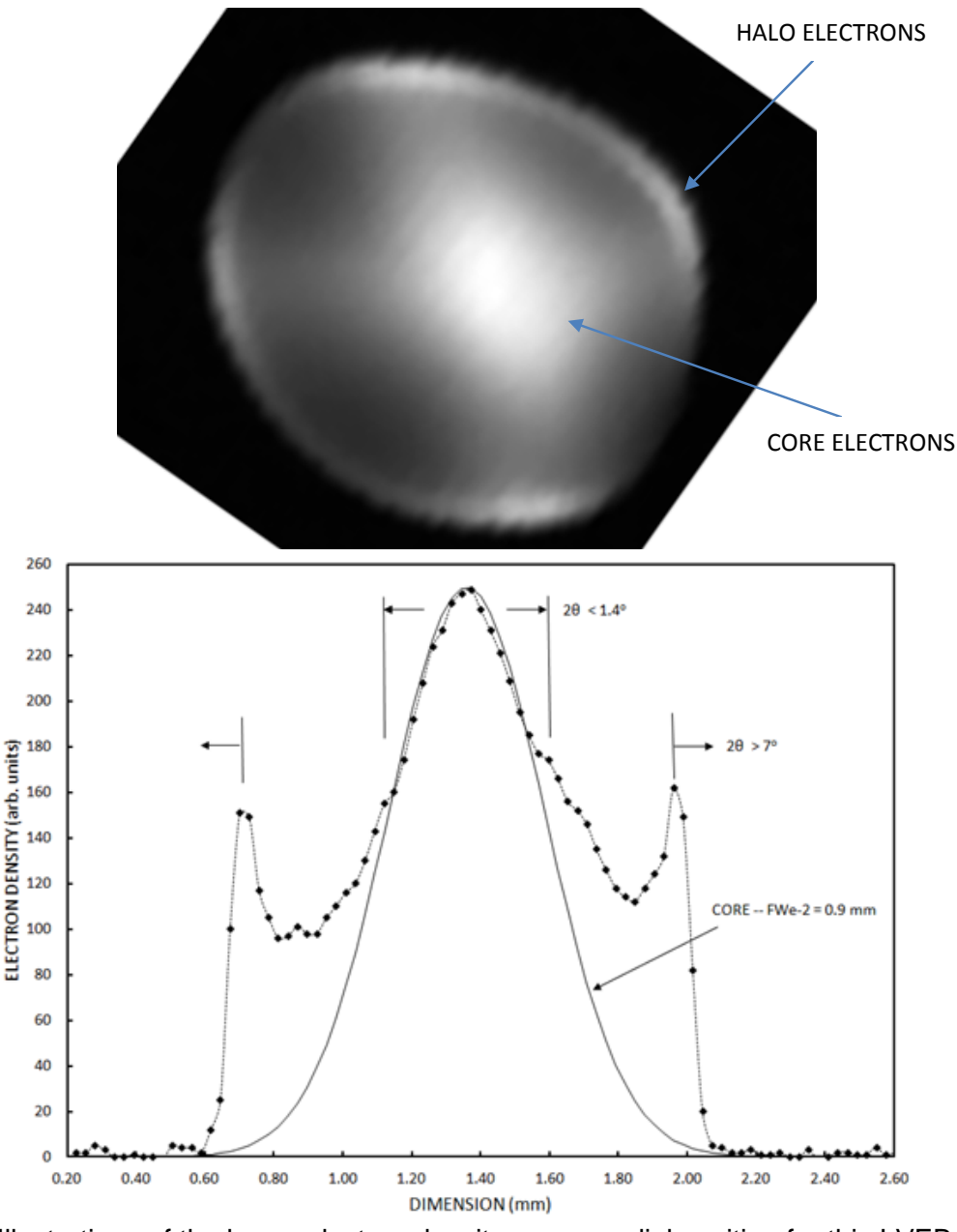


Figure 20: Illustrations of the beam electron density versus radial position for this LVEB machine. These data were obtained with beam parameters: high voltage = 60kV; beam current = 60 mA; work height = 100 mm; focus = -50 underfocus. The angle ranges shown illustrate the relative convergence angles of the core and halo electrons.

An additional important point about the Figure 20 is how the value of D_{2M} compares to the details of the beam shape in this case. For this particular set of beam parameters and this degree of defocus it turns out that the PBD determined beam size is $D_{2M} \approx 1.4$ mm. Looking at the raw data shown in Figure 20 it is apparent that the second moment calculation of beam diameter returns a value that is dominated by the diameter of the roughly 20% of the electrons in the halo of the beam. Recall that this is no surprise since the electron density is weighted by the square of the distance of those electrons, r^2 , from the beam center. A small fraction of electrons substantially removed from the core thereby dominate the D_{2M} value. In other words, this demonstrates that the second moment calculation of beam diameter does not properly represent the important core beam power density for this LVEB.

An additional important question is: how is it that the core power density can come to its minimum diameter at a value different than the minimum in D_{2M} ? The answer is that the core and halo electrons approach sharp focus with different convergence angles and do arrive at their respective minima at different vertical heights in the beam. In order to quantify this effect, the core and halo diameters were measured from the PBD raw data as a function of focus coil current. Knowing the correspondence of focus coil current to vertical position, the relative convergence angles of the two populations of electrons can be determined. The results of that analysis is illustrated in Figure 21. The basic result of this analysis is: the halo electrons approach their minimum at a convergence angle of $2\theta \approx 7^\circ$ with their minimum at $F \approx 1905$ while the core electrons approach their minimum at a convergence angle of $2\theta \approx 1.4^\circ$ with their minimum at $F \approx 1925$. Therefore, the minimum in D_{2M} will occur at about F = 1910 while the peak power density will occur at about F = 1925 (which is the value most relevant to weld penetration in the Ta-10W alloy). This picture of the beam is consistent with the weld results.

An additional corroborating bit of information in this regard was provided to us courtesy of ProBeam. In this case ProBeam generated an interesting direct image of the beam versus focus coil current by sweeping the beam across the PBD aperture while automatically sloping the focus coil current from underfocus through sharp to overfocus. The resulting beam picture relevant to this LVEB is shown in Figure 22. This picture confirms that the core and halo electrons arrive at their respective minimum dimensions at different vertical heights in the beam. Since the measured beam diameter given as D_{2M} is most closely tied to the halo electrons, the minimum in D_{2M} is seen to occur at about the minimum in the halo dimension while the maximum weld penetration in the Ta-10W alloy (depending mostly on the higher power density core electrons) would occur more nearly at the minimum in the core dimension, which corresponds to an apparent beam overfocus. Again, this is entirely consistent with the observed weld penetration behavior.

All of this re-analysis of the beam profiling data illustrates the extent to which the second moment calculation of beam diameter, D_{2M} , does not adequately describe all of the important properties of the beam for this LVEB machine. The fact that the beam has "core" and "halo" components is somewhat unique to the gun design used on this machine and is, therefore, a bit unique to this machine. Nevertheless, a different definition of beam diameter more directly tied to the beam power density would seem to be a better quantity when applied to this application.

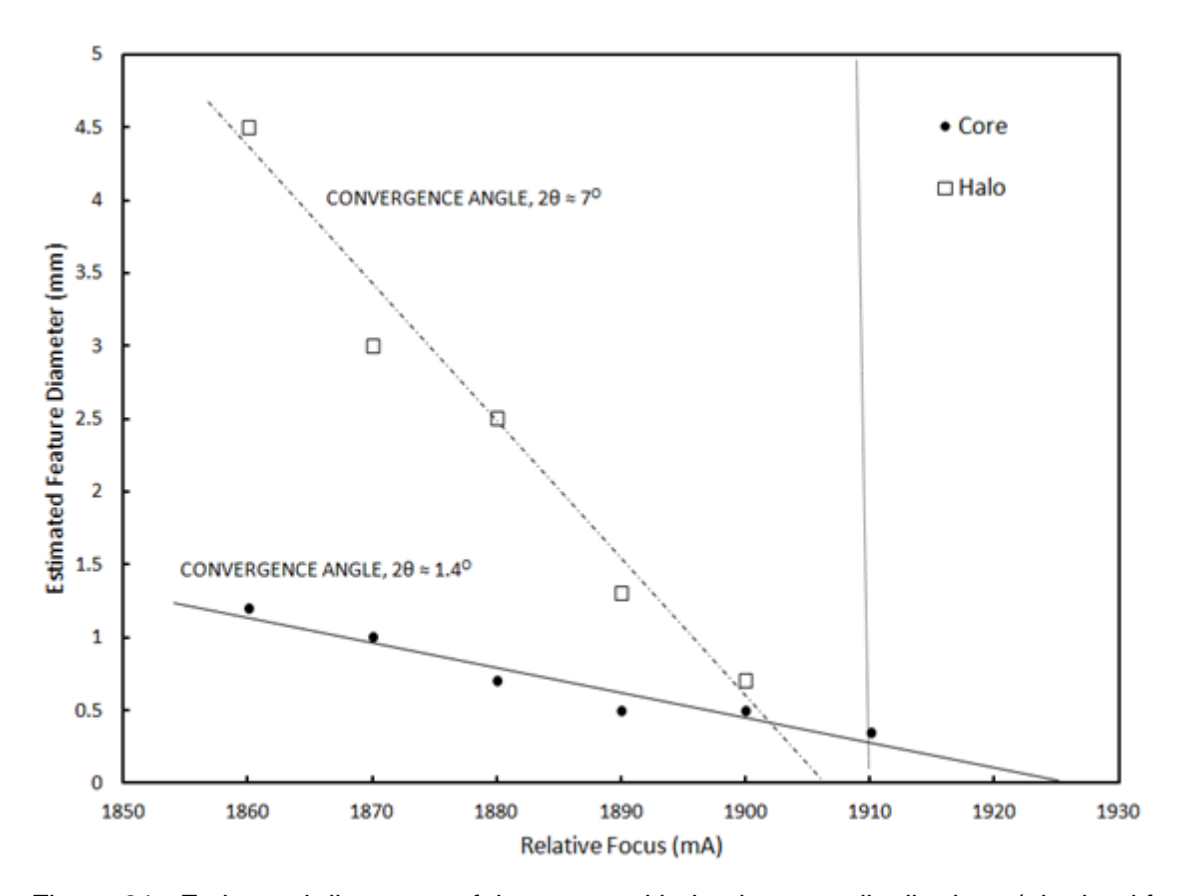


Figure 21: Estimated diameters of the core and halo electrons distributions (obtained from analysis of the PBD beam images) versus focus. These data were obtained with beam parameters: high voltage = 60kV; beam current = 60 mA; work height = 100 mm.

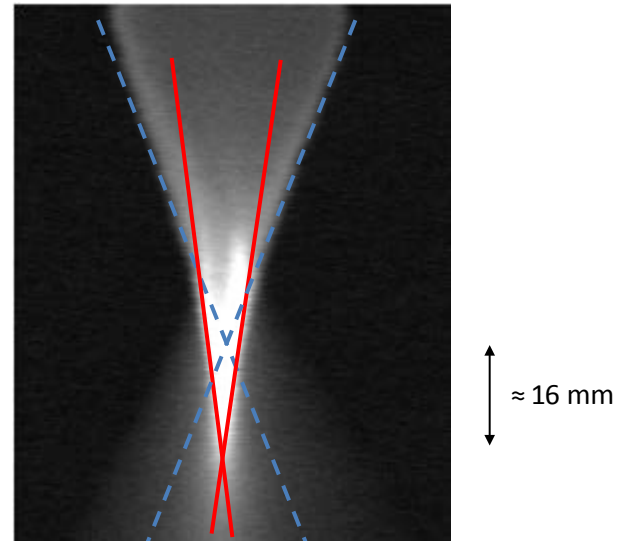


Photo courtesy of Pro-Beam

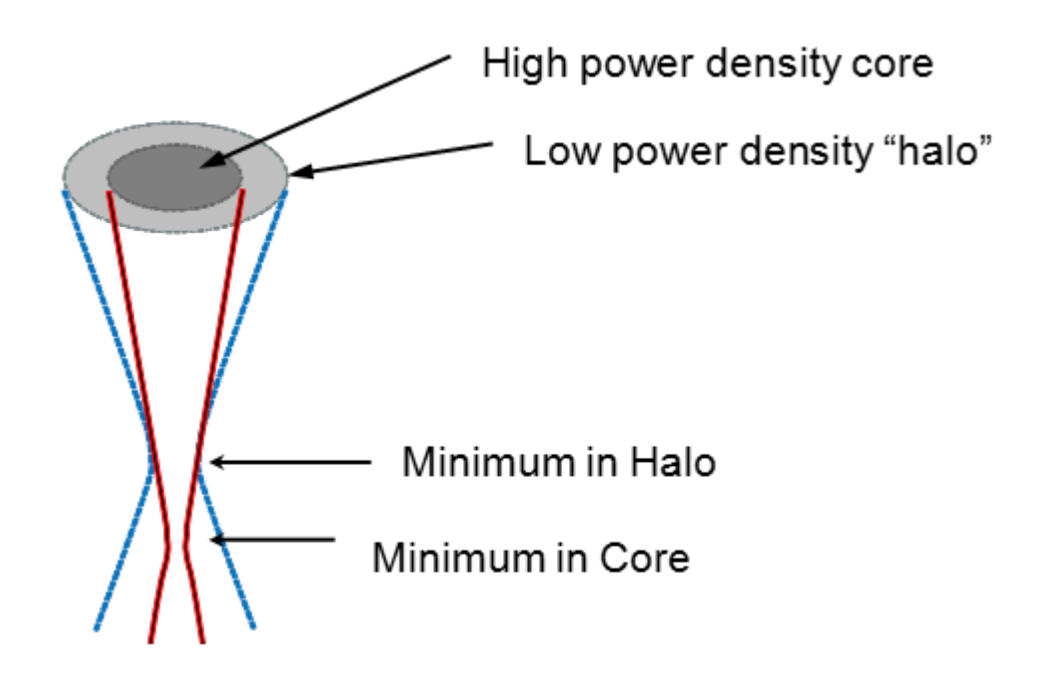


Figure 22: Picture of the beam in a Pro-Beam LVEB machine. The accompanying schematic diagram clarifies what we believe the picture is showing. An offset in heights of the core sharp focus and the overall minimum dimension of the beam is seen to be the case for this machine.

Detailed Analysis of PBD Data - Additional Data for Beam Shape

It does seem that the interesting discrepancy between the measured sharp focus point and maximum weld penetration in the Ta-10W material is understandable based on the complex shape of the beam from this LVEB and the difference between the D_{2M} minimum point and the point of maximum beam power density. We do believe that this interpretation of all of the results from this study is correct. However, in order to be rigorously honest we must point out an interesting problem with the beam profiling data.

We have postulated that the weld data are consistent with the beam consisting of a high power density core surrounded by a reasonably diffuse halo and that those two populations of electrons pass through their respective minima at different focus coil current values. If this hypothesis is valid, the PBD profiler raw data of beam electron density versus position in the beam should show those features.

Detailed analysis of the beam profile data is a bit difficult because the PBD software does not actually return the electron density information in an accessible fashion. What we actually can access from the PBD software is an image file of the sort shown in Figure 19. This is a map of the beam with brightness in any pixel being limited to 256 gray-scale values. We must assume that those image brightness values correspond correctly to actual electron density. Another issue related to the image file is that it is difficult to even obtain the gray-scale values in the image. One can interrogate the image file to obtain a map of the gray-scale brightness values along a particular direction in the image. That is why the data we will discuss here is actually showing the brightness values along only four particular directions in that image.

Figure 23 – 25 show our efforts to retrieve the PBD data for three beam focus conditions. Figure 23 shows data for F = 1910, the apparent sharp focus. Here the beam is nicely circularly symmetric and Gaussian in nature. The best fit to those data is FWe-2 = 0.36 mm, which is essentially identical to the D_{2M} returned by the PBD software for that beam. Figure 24 shows data for +10 overfocus. Here we again see a nearly Gaussian beam shape with is FWe-2 = 0.37 mm, which is a bit different from $D_{2M} = 0.45$ mm but the agreement is acceptable. Perhaps most significantly Figure 24 does show evidence of a beam core with FWe-2 ≈ 0.25 mm, which is consistent with our hypothesis about the beam core becoming narrower for some overfocus. If our hypothesis about the beam behavior is correct, the Figure 15 data for +20 overfocus is most significant. We have proposed that the +20 over focus data should have a low power density halo roughly 1 mm in diameter and a high power density core with a diameter of roughly 0.3 mm. However, that does not seem to be the case. Figure 25 shows electron density versus radial position in the beam at the appropriate overfocus. As can be seen, the data are reasonably Gaussian in nature and are fit reasonably well by FWe-2 = 0.8 mm, which agrees fairly well with the PBD measured value of $D_{2M} = 0.7$ mm. However, as can be seen, there is no apparent narrow feature in the beam that correspond to the presumed high power density in the beam core. The dashed line on Figure 23 is data from a slice through the beam called "vertical", which does suggest the possibility of a beam feature in that direction having a width of perhaps 0.4 mm. However, the lack of an obvious high power density beam core may indicate that our interpretation of the weld results is simply wrong.

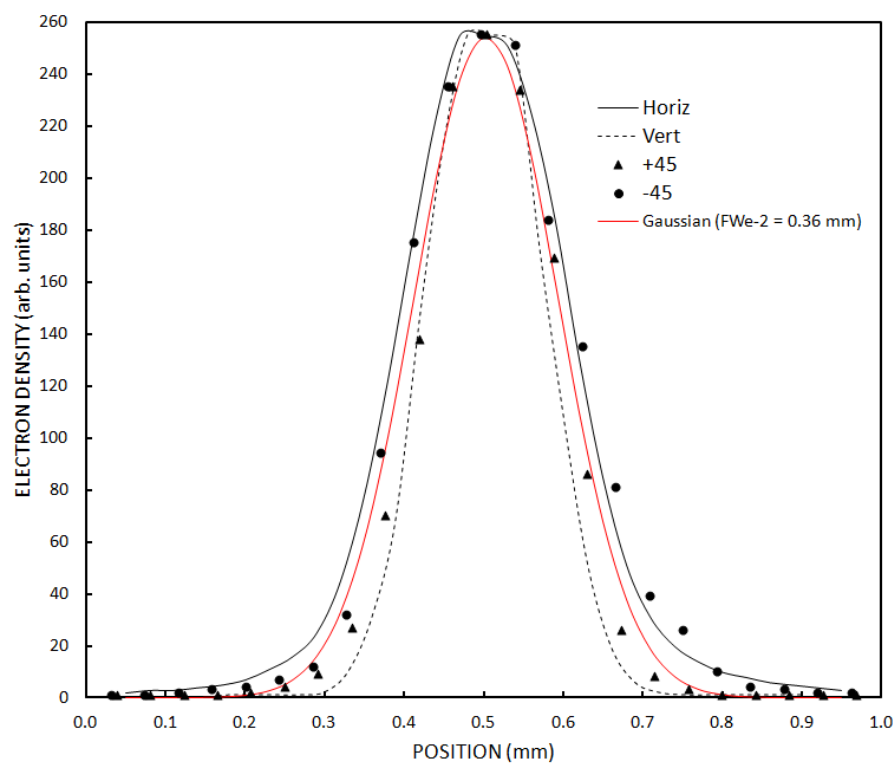


Figure 23: Electron density versus position measured at F = 1910 (apparent sharp focus). The red line shows the best-fit Gaussian curve with FWe-2 = 0.36 mm.

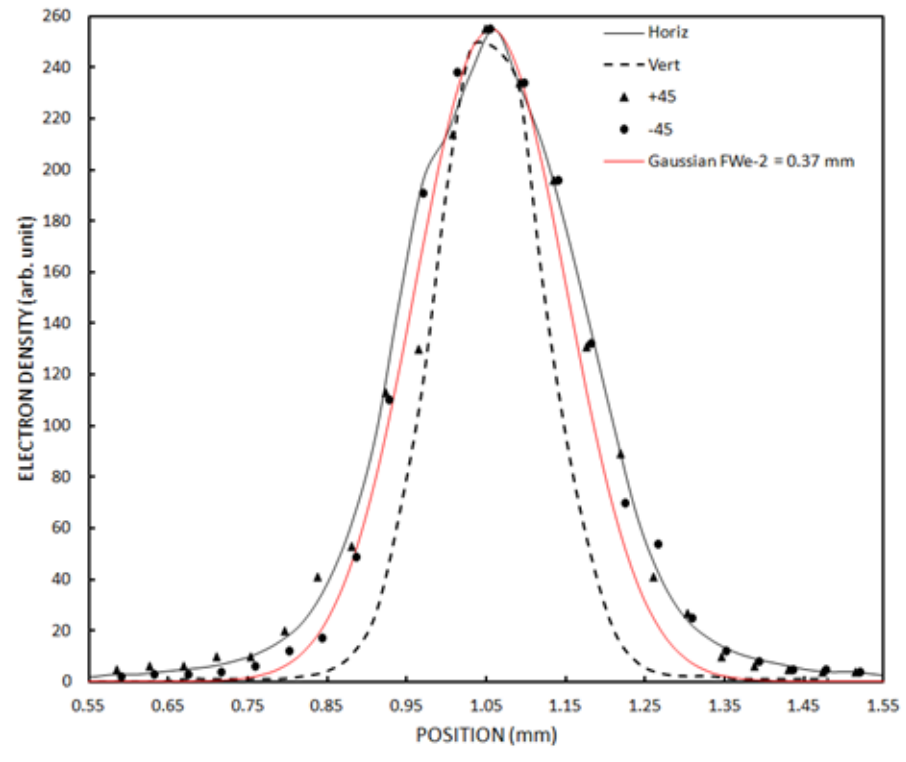


Figure 24: Electron density versus position measured at F = 1920. The red line shows the best-fit Gaussian curve with FWe-2 = 0.37 mm. Note that the vertical slice through the beam is consistent with a Gaussian distribution having FWe-2 = 0.25 mm.

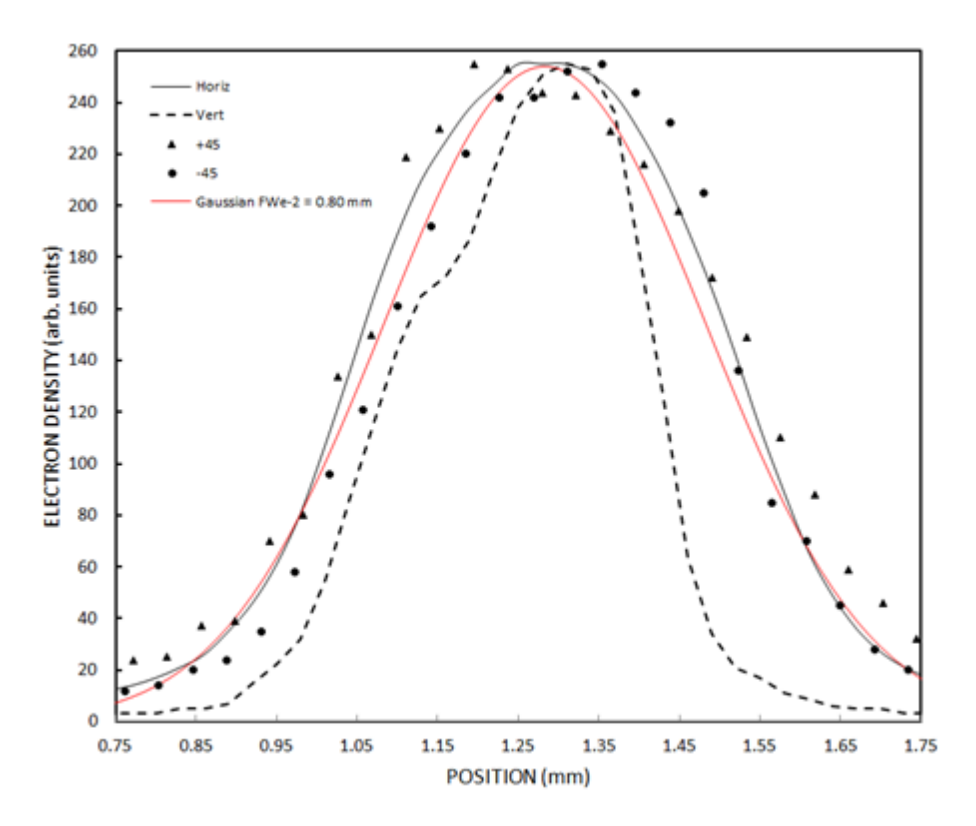


Figure 25: Electron density versus position measured at F = 1930. The red line shows the best-fit Gaussian curve with FWe-2 = 0.8 mm.

There are some experimental complications to the PBD data that might contribute to the discrepancy between the weld results and the beam profiling.

One problem is that the PBD software only allows us access to the image file of the sort shown in Figure 19. We must assume that these brightness values in the image correspond correctly to actual electron density; that may not be the case. Since this an image of the beam it is possible that the image contrast has been adjusted by the software such that a particular pixel gray-scale value does not correspond to the actual electron density. It is certain that the PBD software uses a fairly complex algorithm to adjust the image contrast and background in order to achieve a useful image of the beam. It is possible that algorithm inadvertently discards the high electron density information we were seeking.

Another possible reason why the PBD beam profiling data don't show the beam core might be related to a limitation of any such beam profiling device. If the input aperture to the device is comparable in size to the beam diameter, the data from the profiler will be in error. In this experiment the PBD aperture diameter was measured to be 0.14 mm. Thus, any feature of the beam comparable to that size will not be properly detected. An example of the resulting possible error is shown in Figure 26. This represents a numerical simulation of a Gaussian beam with a true diameter of FWe-2 = 0.14 mm passing across a circular aperture with diameter of 0.14 mm. The symbols on Figure 26 are the simulated signal that would come from the PBD

as the beam passes across the aperture in one linear direction of movement. As can be seen, the beam with an actual diameter equal to the aperture size would be detected as a nearly Gaussian beam with an apparent diameter that is significantly larger than the correct value. A series of these numerical simulations showed that any feature in the beam with FWe-2 < 0.2 mm will simply never be detected by the PBD with its relatively large aperture size. Thus, it is possible that the postulated high power density core of the beam does exist but that the PBD cannot detect it properly. That would only be relevant if the core at its minimum has a size FWe-2 \approx 0.2 mm, which seems is at least somewhat possible based on the weld shape data discussed previously.

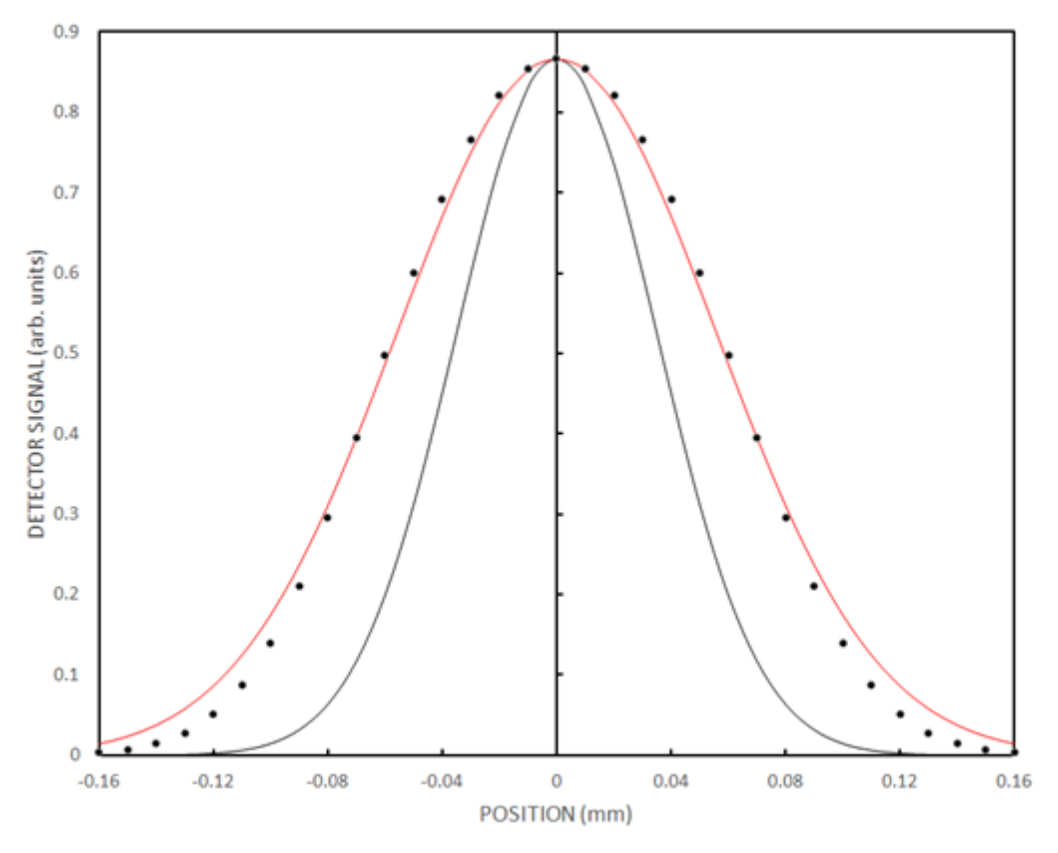


Figure 26: Results from numerical modeling of a Gaussian beam passing across a circular aperture. In this model it was assumed that the aperture diameter is 0.14 mm. The black curve is the starting Gaussian beam model with $D_{2M} = 0.14$ mm. The simulated signal from the PBD, shown as the symbols, is fit fairly well by $D_{2M} = 0.23$ mm, the red curve.

The Problem with D_{2M} – Additional Numerical Simulations

The primary purpose of this section of this paper is to present some numerical simulations of the presumed beam shape of this ProBeam LVEB machine which help elucidate how the present definition of beam diameter, D_{2M}, can be quite misleading. These simulations are based on the basic beam shape shown in Figure 16, which is that the beam is a Gaussian shaped core surrounded by a roughly circular halo of electrons.

For a simple Gaussian shaped beam FWe-2 and D_{2M} are identically the same. However, it is possible that a more complex beam shape, such as seen in this particular machine, could result in the two diameter values being substantially different. The basic reason for this is that the second moment computes E(r) r^2 so that a relatively small number of electrons at a large value of r will substantially affect the diameter calculation. Figure 27 illustrates this point. Here we have made a numerical model of a hypothetical beam consisting of a Gaussian core surrounded by a ring. Completely arbitrarily it was assumed that the diameter of the ring was 1.75 and the Gaussian core had FWe-2 = 0.8 in arbitrary units. In this particular model 10% of the electrons are in the ring. A least-squares Gaussian fit to the data gives FWe-2 = 0.82 and a calculation of second moment yields $D_{2M} = 1.2$ (arb. units). This illustrates the point that a few percent of the electrons outside of the beam core can easily result in a large difference in the computed diameter values depending on how far those electrons are from the beam centroid. Further, it is clear that the D_{2M} value may well not be at all indicative of the high power density core of the beam and can be more nearly representative of the diameter of the outlying electrons.

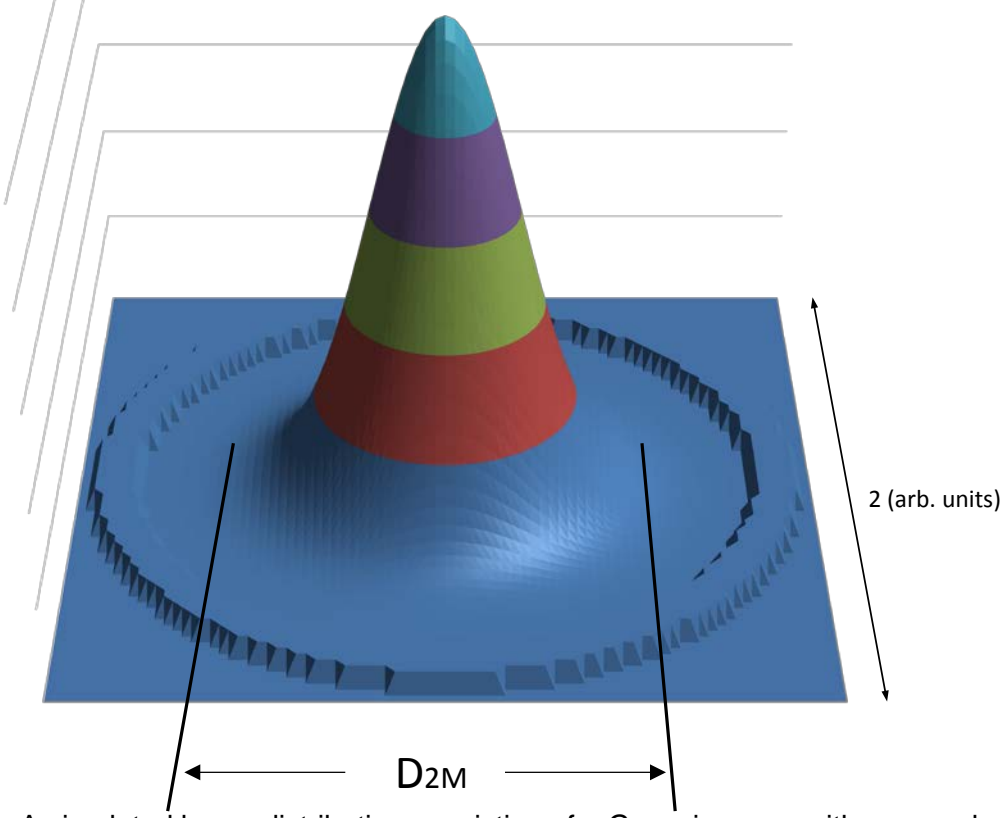


Figure 27: A simulated beam distribution consisting of a Gaussian core with an annular ring around that core (similar to what is seen in this machine). In this case, 10% of the beam electrons are in the ring and the calculations yield: FWe-2 = 0.8 and D_{2M} = 1.2 (arb. units).

The ring model was used to gain further insight into how the PBD data for D_{2M} could disagree with the weld results. Some details of the model must be discussed. First, the model was built assuming a Gaussian core whose diameter was read from Figure 21. It was assumed that this core passes through its minimum diameter at F 1930. Second, the ring was assumed to have a constant width of 0.2 mm, which is roughly consistent with data in Figure 20. The details of the ring actually proved unimportant, but what is critical is the ring diameter and the fraction of total electrons in the ring. The ring diameter was read from Figure 21 and it was assumed that the ring electrons pass through their minimum diameter at F 1910. It is also assumed that the divergence behavior of the two populations of electrons is the same as their convergence behavior, which should be the case even if not obvious from the raw data. The third crucial aspect of the numerical model is the assumption of what fraction of the electrons are in the "halo" relative to the core. It turns out that a very good match to the PBD measured values for D_{2M} results if the "halo" is assumed to contain a constant 10% of the total electrons. Considering profiling data such as shown in Figure 20, the 10% value seems realistic. Results from the numerical model using the aforementioned assumptions are shown in Figure 28.

The basic result from these numerical simulations is that the measured beam diameter, and especially the beam diameter given as D_{2M} , would have a strong tendency to be minimum where the more highly converging "halo" electrons pass through their minimum. It is also clear that the beam maximum power density occurs where the "core" electrons are at their minimum diameter and that beam condition is not represented at all by the D_{2M} value. These numerical results agree qualitatively with the weld penetration data versus beam focus especially for the Ta-10W alloy (presumably because of its thermos-physical properties, which make the weld behavior of this material unusually sensitive to beam power density).

All research on this subject has led to the basic conclusion that weld keyhole behavior (weld penetration and width) is mostly closely linked to the high power density core of the beam. Therefore, the value of D_{2M} could be misleading in this regard because its calculation methodology more strongly weights electrons outside of the beam core. As the "core" and "halo" electrons converge and diverge while passing through sharp focus, D_{2M} values may well not properly capture the location where the high power density core of the beam passes through its minimum (D_{2M} would tend to indicate where the "halo" electrons pass through minimum). These results help show that a different method of calculating beam diameter, and one which better describes the beam power density especially at the beam core, might be helpful for better predicting weld behavior of this machine with its somewhat unusual beam shape. It should be noted that the alternative beam diameter definition that has been used in the past, FWe-2, does actually seem to be more descriptive of weld behavior because it is more indicative of the assumed Gaussian core. However, actual experimental beam profile data tended to show little difference between D_{2M} and FWe-2 for those experimental results. This leads to the conclusion that an entirely different approach to determining beam diameter might be necessary.

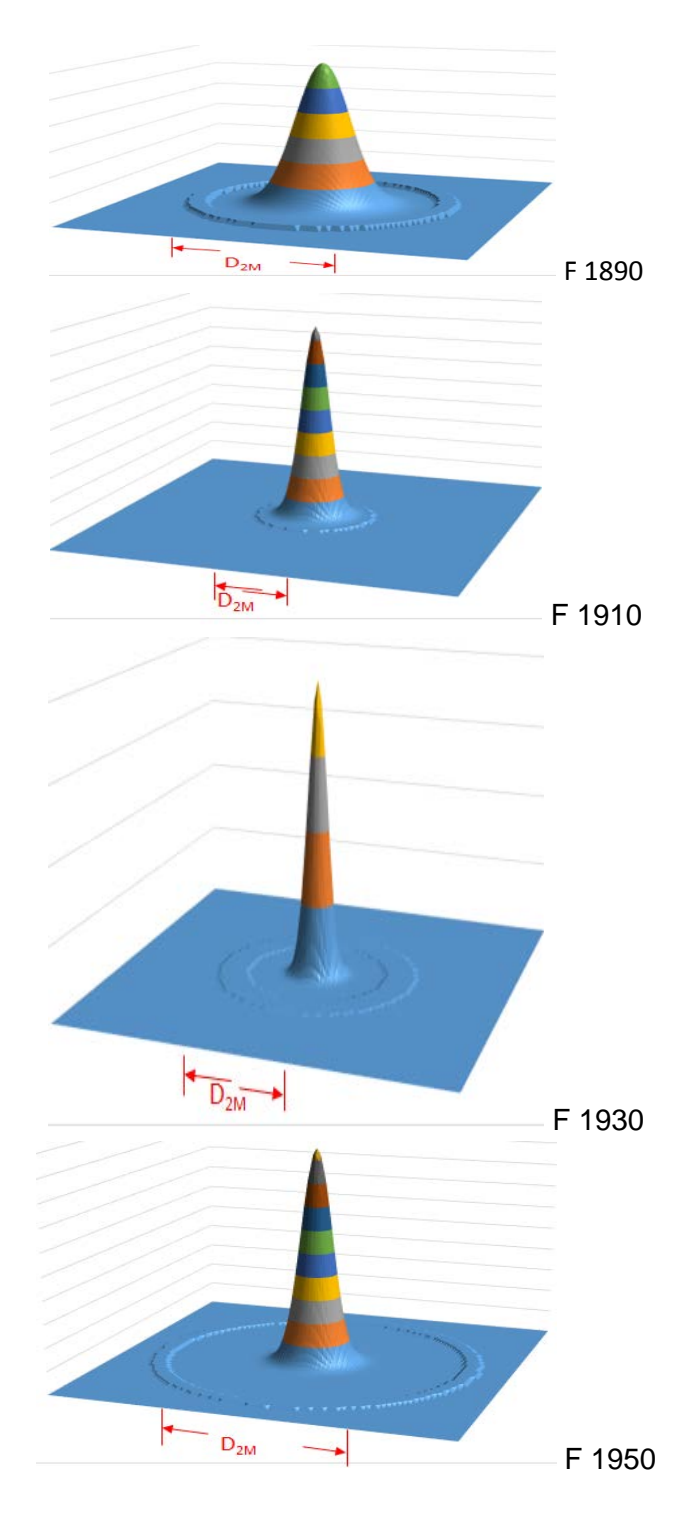


Figure 28: Numerical simulations of a beam consisting of a Gaussian core with a "halo" consisting of 10% of the electrons. The values of D_{2M} computed from this model agree with the PBD data and show that the measured beam diameter responds most strongly to the "halo" diameter while the peak power density of the beam is dominated by the Gaussian core.

CONCLUSIONS

Historically it has proven useful to measure the electron beam current density (beam profiling) in the beam produced by electron beam welding machines. The measured diameter of the beam was found to correlate well with the depth of penetration and keyhole width of the resulting welds. Historically the beam diameter has largely been defined as a measurement of the width of the nearly Gaussian shaped beam and often been given as FWe-2. It is also possible to compute the second-moment diameter of the beam, and D_{2M} , which is essentially equally useful for the typical high voltage EB machines mostly studied in the past.

Recently LANL acquired two low voltage EB machines from Pro-Beam and the notion of beam profiling was applied to those machines. As part of a weld development effort associated with welding of a Ta-10W alloy, measured beam diameter was correlated with the resulting welds. It was discovered this LVEB has a somewhat unusual beam shape because of its gun design. Most importantly, it was found that the measured diameter of the beam (D_{2M} in this particular case) did not correlate well with the weld dimensions, especially for the Ta-10W results.

A detailed analysis of the weld results revealed that the beam from this LVEB machine consists of two populations of electrons, a high power density "core" and a more diffuse "halo". The basic reason that the measured beam diameter does not correlate with the weld dimensions is that the weld is most responsive to the high power density "core" while the D_{2M} values are most sensitive to the diffuse "halo" of electrons. Thus, the existing ways of describing beam diameter for this machine are inadequate.

The results presented in this paper suggest that a different way to define the beam diameter measurement might be useful to EB welding. That new beam diameter definition should be an analysis methodology that yields a result that is more descriptive of the high power density portion of the beam. Additionally, the data suggest that a proper definition of beam diameter may have to include some dependence on the thermal properties of the material being welded.